NOAA Technical Report NESS 89

A Statistical Approach to Rainfall Estimation Using Satellite and Conventional Data

Washington, D.C.
April 1982

U.S. DEPARTMENT OF COMMERCE
National Oceanic and Atmospheric Administration
National Earth Satellite Service

NOAA TECHNICAL REPORTS

National Earth Satellite Service Series

The National Earth Satellite Service (NESS) is responsible for the establishment and operation of the environmental satellite systems of NOAA.

Publication of a report in NOAA Technical Report NESS series will not preclude later publication in an expanded or modified form in scientific journals. NESS series of NOAA Technical Reports is a continuation of, and retains the consecutive numbering sequence of, the former series, ESSA Technical Report National Environmental Satellite Center (NESC), and of the earlier series, Weather Bureau Meteorological Satellite Laboratory (MSL) Report. Reports 1 through 39 are listed in publication NESC 56 of this series.

Reports in the series are available from the National Technical Information Service (NTIS), U.S. Department of Commerce, Sills Bldg., 5285 Port Royal Road, Springfield, VA 22161, in paper copy or microfiche form. Order by accession number, when given, in parentheses. Beginning with 64, printed copies of the reports, if available, can be ordered through the Superintendent of Documents, U.S. Government Printing Office, Washington, DC 20402. Prices given on request from the Superintendent of Documents or NTIS.

ESSA Technical Reports

NESC 46 Monthly and Seasonal Mean Global Charts of Brightness From ESSA 3 and ESSA 5 Digitized Pictures, February 1967-February 1968. V. Ray Taylor and Jay S. Winston, November 1968, 9 pp. plus 17 charts. (PB-180-717)

NESC 47 A Polynomial Representation of Carbon Dioxide and Water Vapor Transmission. William L. Smith, February 1969 (reprinted April 1971), 20 pp. (PB-183-296)

NESC 48 Statistical Estimation of the Atmosphere's Geopotential Height Distribution From Satellite Radiation Measurements. William L. Smith, February 1969, 29 pp. (PB-183-297)

NESC 49 Synoptic/Dynamic Diagnosis of a Developing Low-Level Cyclone and Its Satellite-Viewed Cloud Patterns. Harold J. Brodrick and E. Paul McClain, May 1969, 26 pp. (PB-184-612)

NESC 50 Estimating Maximum Wind Speed of Tropical Storms From High Resolution Infrared Data. L. F. Hubert, A. Timchalk, and S. Fritz, May 1969, 33 pp. (PB-184-611)

NESC 51 Application of Meteorological Satellite Data in Analysis and Forecasting. Ralph K. Anderson, Jerome P. Ashman, Fred Bittner, Golden R. Farr, Edward W. Ferguson, Vincent J. Oliver, Arthur H. Smith, James F. W. Purdom, and Rance W. Skidmore, March 1974 (reprint and revision of NESC 51, September 1969, and inclusion of Supplement, November 1971, and Supplement 2, March 1973), pp. 1--6C-18 plus references.

NESC 52 Data Reduction Processes for Spinning Flat-Plate Satellite-Borne Radiometers. Torrence H. MacDonald, July 1970, 37 pp. (COM-71-00132)

NESC 53 Archiving and Climatological Applications of Meteorological Satellite Data. John A. Leese, Arthur L. Booth, and Frederick A. Godshall, July 1970, pp. 1-1--5-8 plus references and appendixes A through D. (COM-71-00076)

NESC 54 Estimating Cloud Amount and Height From Satellite Infrared Radiation Data. P. Krishna Rao, July 1970, 11 pp. (PB-194-685)

NESC 56 Time-Longitude Sections of Tropical Cloudiness (December 1966-November 1967). J. M. Wallace, July 1970, 37 pp. (COM-71-00131)

NOAA Technical Reports

NESS 55 The Use of Satellite-Observed Cloud Patterns in Northern Hemisphere 500-mb Numerical Analysis. Roland E. Nagle and Christopher M. Hayden, April 1971, 25 pp. plus appendixes A, B, and C. (COM-73-50262)

NESS 57 Table of Scattering Function of Infrared Radiation for Water Clouds. Giichi Yamamoto, Masayuki Tanaka, and Shoji Asano, April 1971, 8 pp. plus tables. (COM-71-50312)

NESS 58 The Airborne ITPR Brassboard Experiment. W. L. Smith, D. T. Hilleary, E. C. Baldwin, W. Jacob, H. Jacobowitz, G. Nelson, S. Soules, and D. Q. Wark, March 1972, 74 pp. (COM-72-10557)

NESS 59 Temperature Sounding From Satellites. S. Fritz, D. Q. Wark, H. E. Fleming, W. L. Smith, H. Jacobowitz, D. T. Hilleary, and J. C. Alishouse, July 1972, 49 pp. (COM-72-50963)

NESS 60 Satellite Measurements of Aerosol Backscattered Radiation From the Nimbus F Earth Radiation Budget Experiment. H. Jacobowitz, W. L. Smith, and A. J. Drummond, August 1972, 9 pp. (COM-72-51031)

(Continued on inside back cover)

NOAA Technical Report NESS 89

A Statistical Approach to Rainfall Estimation Using Satellite and Conventional Data

Linwood F. Whitney, Jr.

Washington, D.C.
April 1982

U.S. DEPARTMENT OF COMMERCE
Malcolm Baldrige, Secretary

National Oceanic and Atmospheric Administration
John V. Byrne, Administrator

National Earth Satellite Service
John H. McElroy, Assistant Administrator for Satellites

CONTENTS

TABLES

FIGURES

A STATISTICAL APPROACH TO RAINFALL ESTIMATION USING SATELLITE AND CONVENTIONAL DATA

Linwood F. Whitney, Jr.
Earth Satellite Laboratory
National Earth Satellite Service
National Oceanic and Atmospheric Administration
Washington, D. C.

ABSTRACT. A statistical approach is employed in an attempt to estimate convective rainfall using both satellite and conventional data. The objective is to provide rainfall estimates in a form suitable as input to hydrologic models which forecast riverflow.

A variety of variables derived from both satellite and conventional meteorological sources are included in the study. All variables are thought to be potentially related, either physically or empirically, to the rainfall process. From among these variables, a screening regression method selects those which best explain area-averaged rainfall.

Among the cases studied, the relationship of each variable to rainfall is weak to poor, particularly as cases are combined. Although multivariate selections improve the relationships, inconsistency of selection develops from one case to another and from one time to another, even in the same meteorolgical situation. Regression equations are found to estimate the amount inadequately, even when using dependent data. These facts led to the conclusion that, at best, rainfall is not likely to be measured quantitively by such an approach and, at worst, concern is raised about the validity of using the variables investigated to estimate rainfall.

An IR threshold temperature of $0^{o}C$ is found to effectively separate instances of rain from no rain. Even this result is tempered by the fact that all cases selected were over rather confined areas during select periods of active convection and rainfall. Given less vigorous convection but with cloud tops above the freezing level, an entirely different result may occur.

1. INTRODUCTION

This study was undertaken with the intent of developing a computerized operational scheme for estimating convective rainfall using satellite data. Specifically, the objective was to provide rainfall estimates in a form suitable for input to hydrologic models which forecast riverflow. These models require area-averaged rainfall over periods of 6 hr or more in watersheds covering at least 500 square miles -- a time and space scale larger than normally associated with flash flooding.

The estimation of rainfall using satellite data is an idea of long standing. Many, including Lethbridge (1967), Barrett (1970), Gruber (1973), Follansbee (1976), Scofield and Oliver (1978). Griffith, Woodley, et. al. (1978), and Arkin and Richardson (1979), have presented schemes for doing so. Without reviewing all of these works, it is sufficient to note that although they are fundamentally similar in concept, they vary in approach, purpose, and degree of objectivity. All stem from and to some degree depend on the concept that the coldest and visually brightest convective cloud tops are related to the heaviest rain. The method explored in the present study is no different in this respect. Although the previous works employ many useful approaches and ideas, no one seemed entirely suited to the objective of this study; therefore, a somewhat different course was pursued.

2. APPROACH DEVELOPMENT

For purposes of this study, the advantages of satellite infrared data outweigh those of visible data. Even though the resolution of visible data is eight times greater than IR, and despite long-standing opinion and early evidence of Lethbridge (1967) that visible and IR data together better define convective towers and rainfall probability than either separately, heavy rain occurs most frequently at night (Maddox, Chappell, and Hoxit, 1979). As a result, only IR data were included in this study. These data are available day or night and provide estimates of cloud height.

Although it appears logical that the concentration of large water drops should be at or near the main convective towers which in turn should be identifiable in the infrared views as the coldest spots, the concept, as expected, is somewhat simplistic. The earliest experiment in this study demonstrated a rather weak correlation of satellite IR (infrared) black-body temperature with point observation of rainfall and, later, even with area-averaged rainfall.

These results pointed to the necessity for using information other than IR temperature alone. Many ideas came to mind. Other characteristics of the IR temperature might also be important; the heavy rain, if not always well correlated with the same absolute values of temperature, might instead be better correlated with convective (or cold) cores regardless of the actual temperature or with strongest temperature gradients upstream, downstream, or across-stream of the cores. Also, conventional data might well complement the satellite data and thus serve to refine the convective rainfall estimates. Indeed, any estimation method should take full advantage of any complementary benefit that satellite and conventional data contribute to each other. The methods of Gruber (1973) and Scofield and Oliver (1977) use both conventional and satellite data. Although vastly different in approach, both methods depend heavily upon other meteorological data and logic to supplement cloud-top temperature.

As a result of the rapidly expanding list of ideas to consider and the lack of solid theoretical connection between cloud appearance and rainfall, a purely statistical approach to rainfall estimation was taken. Not only was such an approach unexplored, but it provided an objective means of comparing and testing the variables stemming from the variety of ideas.

Moreover, if such an approach was to evolve into a useful operational technique, objectivity could be helpful. Rainfall estimates must be timely to be useful as input to an operational system which forecasts riverflow. Objectivity in the scheme would provide both the ability to handle large quantities of data from different sources quickly and with consistency and to provide quantitative output in a format for automatic ingestion into the forecast system.

A screening-regression technique was used to develop an equation of variables best defining or correlating with rainfall. This technique generates a series of equations or statistical models such that each model increases by one the number of variables comprising the previous model. In effect, the regression yields the best one-term model, two-term model, etc. Then, from this series, the statistically most significant model is chosen.

Two regression techniques were tried -- maximum variance improvement and residual correlation. In the first technique, each statistical model is selected independently of all other models. In any given model, the prescribed number of variables are selected to achieve the greatest reduction in variance over any other combination of the same number of variables, regardless of selections in other models.

The second technique, the residual correlation, selects for the first statistical model the one variable correlating best with rainfall. Then the next model selects a second variable which correlates best with unexplained or residual rainfall. This procedure is repeated for a three-term model, a four-term model, etc., but it always selects a new variable which best explains the residual rainfall from the previous model. Then, for any given model, the residual method includes all variables previously selected plus a new variable. As new variables are added to successive models, only the constant changes and the coefficients of previously selected variables remain unchanged. In contrast, the maximum variance improvement technique permits the variables and coefficients to vary.

For this study the residual correlation method was chosen, even though the variance reduction method always yielded a higher correlation coefficient (lower variance) at any given model step. The choice, although somewhat arbitrary, was made because the residual method appeared to be less sensitive to possible intercorrelations among variables. Another reason was that there were at times wild fluctuations in the selections by the variance reduction method from one model step to another, while the residual method behaved in a steady, predictable manner.

With this decision made, the final step was to select from the series of models the one most representative of the data sample. The procedure adopted was simply to select the model composed of the maximum number of variables which also showed a statistically significant increase in correlation over the model in the previous step.

The approach, then, was to apply the regression method to the cases selected and to establish whether these statistical relationships to rainfall were meteorologically and hydrologically meaningful, i.e., whether consistent results were repeatable from one case to another, from one time to another, over different time intervals, or between adjacent areas of the same case. In practice, the technique was applied to both 1-hr and 6-hr rainfall, but always over 6 hr intervals.

3. DATA SOURCES AND TREATMENT

Variables involved in this study were derived from geostationary satellite and conventional data and combinations of the two. All are thought to have physical or empirical potential for relationship to rainfall; a few are based on concepts used in other estimation techniques. Table 1 outlines the nature of these variables and the possible connection of each to rainfall. These points are discussed further in this section and in appendix A.

Hourly rainfall observations by state networks (variable 1, table 1) served as the "ground-truth" data base, both in developing the regression equations and in verifying estimates using independent data. Hourly data were required since it was the purpose here to develop a means of estimating rainfall over periods of up to 6 hr.

Geostationary satellites are invaluable to convective studies such as this. The GOES (Geostationary Operational Environmental Satellites) series provide the repeated and frequent coverage (at least every one-half hr) necessary to observe the rapid cloud changes associated with convection. Polar orbiting satellites, on the other hand, provide repeated coverage only twice daily. Hourly infrared data taken by GOES East were used in this study. They were involved in variables 2-11. Surface and upper-air meteorological data (involved in variables 6 - 25, table 1) are routinely and readily available from a variety of sources, much more so than either rainfall or GOES data. Hourly rainfall data can take up to 2 yr to become available; the GOES digital archive was, until recently[1], incomplete and difficult to recover and to reprocess into computer compatible form. Terrain heights of hourly and daily rainfall stations were used to establish the terrain fields needed in variables 26-28 of table 1.

Radar data, although highly desirable, were not used. Since the number of computer digitizing radars in the United States is limited, the coverage of potential rainfall cases would have been severely restricted. No manually digitized radar data were used either, mainly because of concern about its objectivity and therefore its quality.

To establish a statistical relationship between ground truth and each of the independent variables, a grid format is used rather than the format of individual and unique watersheds employed by River Forecast Centers (RFC) (Hydrologic Research Laboratory, 1972) in their operations. The irregular shape and size of watershed seemed a handicap to the mechanics of relating rainfall to the variables over the advantage afforded by the regularity of a grid.

---

[1] GOES data tapes are archived at the Space Science and Engineering Center at the University of Wisconsin, and digital tapes of up to 16 sectors may be ordered through NOAA, Environmental Data and Information Service, Satellite Data Services Division, OA/D56, World Weather Building, Washington, D. C. 20233.

Table 1.--List of variables

NO.	SYMBOL	VARIABLE	FEATURE POTENTIALLY RELATED TO RAIN
1)	R	RAINFALL	"GROUND TRUTH" OR DEPENDENT VARIABLE
2)	C	SATELLITE BLACK-BODY IR TEMPERATURE	COLDEST CLOUD AREAS
3)	$\lvert\nabla C\rvert$	ABSOLUTE IR TEMPERATURE GRADIENT	STRONGEST GRADIENTS
4)	$\nabla^2 C$	LAPLACIAN IR TEMPERATURE	CONVECTIVE CENTERS
5)	$\nabla^2 C/C$	RATIO VARIABLES 4 TO 2	CONVECTIVE CENTERS
6)	$\mathbb{V}_2 \cdot \nabla C/\lvert\mathbb{V}_2\rvert$	TEMPERATURE GRADIENT ALONG 200 MB WIND	HI-LEVEL WINDWARD SIDE OF CONVECTIVE CENTERS
7)	$\mathbb{V}_8 \cdot \nabla C/\lvert\mathbb{V}_8\rvert$	TEMPERATURE GRADIENT ALONG 850 MB WIND	LO-LEVEL WINDWARD SIDE OF CONVECTIVE CENTERS
8)	$\mathbb{V}_{2-8} \cdot \nabla C/\lvert\mathbb{V}_{2-8}\rvert$	TEMPERATURE GRADIENT ALONG TROPOSPHERIC SHEAR	UP-SHEAR SIDE OF CONVECTIVE CENTERS
9)	$C\mathbb{V}_2 \cdot \nabla C/\lvert\mathbb{V}_2\rvert$	PRODUCT OF VARIABLES 2 AND 6	COLDEST PORTION OF HI-LEVEL WINDWARD SIDE OF CONVECTION
10)	$C\mathbb{V}_8 \cdot \nabla C/\lvert\mathbb{V}_8\rvert$	PRODUCT OF VARIABLES 2 AND 7	COLDEST PORTION OF LOW-LEVEL WINDWARD SIDE OF CONVECTION
11)	$C\mathbb{V}_{2-8} \cdot \nabla C/\lvert\mathbb{V}_{2-8}\rvert$	PRODUCT OF VARIABLES 2 AND 8	COLDEST PORTION OF UP-SHEAR SIDE OF CONVECTION
12)	DP_{SFCM}	SURFACE DEWPOINT (MIDTIME)	MOIST AREAS
13)	DP_{SFCS}	SURFACE DEWPOINT (START)	MOIST AREAS
14)	DP_8	850 MB DEWPOINT	MOIST AREAS
15)	$-\mathbb{V}_8 \cdot \nabla DP_{SFCM}$	SURFACE DEWPOINT (MIDTIME) ADVECTION BY 850 MB WIND	STRONGEST MOISTURE ADVECTION
16)	$-\mathbb{V}_8 \cdot \nabla DP_{SFCS}$	SURFACE DEWPOINT (START) BY 850 MB WIND	STRONGEST MOISTURE ADVECTION
17)	$-\mathbb{V}_8 \cdot \nabla DP_8$	850 MB DEWPOINT ADVECTION	STRONGEST MOISTURE ADVECTION
18)	$\mathbb{V}_2 \cdot \nabla DP_{SFCM}/\lvert\mathbb{V}_2\rvert$	SURFACE DEWPOINT (MIDTIME) GRADIENT ALONG 200 MB WIND	HI-LEVEL WINDWARD SIDE OF SURFACE MOISTURE RIDGE
19)	$\mathbb{V}_2 \cdot \nabla DP_{SFCS}/\lvert\mathbb{V}_2\rvert$	SURFACE DEWPOINT (START) GRADIENT ALONG 200 MB WIND	HI-LEVEL WINDWARD SIDE OF SURFACE MOISTURE RIDGE
20)	$\mathbb{V}_2 \cdot \nabla DP_8/\lvert\mathbb{V}_2\rvert$	850 MB DEWPOINT GRADIENT ALONG 200 MB WIND	HI-LEVEL WINDWARD SIDE OF LO-LEVEL MOISTURE RIDGE
21)	$\nabla^2 DP_{SFCM}$	LAPLACIAN SURFACE DEWPOINT (MIDTIME)	MOISTURE CENTERS
22)	$\nabla^2 DP_{SFCS}$	LAPLACIAN SURFACE DEWPOINT (START)	MOISTURE CENTERS
23)	$\nabla^2 DP_8$	LAPLACIAN 850 MB DEWPOINT	MOISTURE CENTERS
24)	θ_{eM}	EQUIVALENT POTENTIAL TEMPERATURE (MIDTIME)	WARM, MOIST AREAS (INSTABILITY)
25)	θ_{es}	EQUIVALENT POTENTIAL TEMPERATURE (START)	WARM, MOIST AREAS (INSTABILITY)
26)	h	TERRAIN HEIGHT	HIGH TERRAIN
27)	$\mathbb{V}_8 \cdot \nabla h/\lvert\mathbb{V}_8\rvert$	TERRAIN GRADIENT ALONG LO-LEVEL WIND	STRONGEST UP-SLOPE MOTION
28)	$\nabla^2 h$	LAPLACIAN OF TERRAIN HEIGHTS	HIGH TERRAIN

A grid interval of 0.3 deg lat.-long. was used. This mesh, although somewhat arbitrarily selected, approximately represents both the average spacing between hourly rainfall stations (appendix B) and an area smaller than the smallest watershed typically defined by the RFC's.

Use of a grid format necessitated the adoption of a different method of area-averaging the rainfall than that used by the RFC's. First, measured rainfall was analyzed by the so-called Weaver method (appendix C) at 0.1 degree lat.-long. grid intervals over an initial grid area of 4.1 deg lat. by 7.4 deg long. Finally, the values in each 3x3 array were averaged to a single value centered at each 0.3-deg grid point within a final grid area of 2.1 deg lat. by 5.4 deg long. These averages were the ground truth used in the regression development.

Any procedure which averages rainfall areally is understandably regarded with skeptism because of the horizontal variability of rainfall. Neither the Weaver nor RFC techniques are exceptions. An experiment to test the compatibility of the two provided evidence (figure 1) that Weaver reasonable approximates the watershed averages of the RFC. In that experiment, 24-hr rainfall was analyzed by the procedure in the previous paragraph. An average of the rainfall at all 0.3 deg grid points falling within each watershed were compared to each RFC average. The comparison in figure 1 shows a correlation of 0.86 and a regression line of a slope near 1 and a small bias. Of the eight comparisons departing most radically from the rest, at least six suffered from sparse gauge density, making the averages of both methods questionable.

IR temperature was also averaged over time and area for correlation to 6-hr, area-averaged rainfall. Each grid-point temperature consists of an average of the values in a three-line by nine-pixel (picture element) array found in all six of the hourly pictures. An IR array of these dimensions represents an area roughly the same as that of an individual grid interval. Time averaging provides some measure of the persistence of cold clouds at given locations. Spatial averaging helps minimize effects of noise found in the 1975 GOES East data and of navigational uncertainties.

Navigation of Earth location of picture pixels was first closely approximated by objective[2] means. A digital printout was then produced from which the computer locations of identifiable landmarks were checked manually against actual locations. Refinements in location, if any, were incorporated by making the appropriate pixel and line shifts of the data to within an estimated 2-pixel uncertainty.

Hourly comparisons were also made within the same 6-hr periods. IR temperatures were averaged areally in the same manner as above except that the averaging was done only on individual hourly pictures (no time averaging) for correlation with the appropriate hourly, area-averaged rainfall.

GOES data were used not only in the screening regression procedure but in the initial discrimination of occurrences of rain from those of no rain. Only

---

[2]The navigation procedure used was that designed by Benjamin Remondi, NOAA/NESS, Information Processing Division, Orbital mechanics Branch.

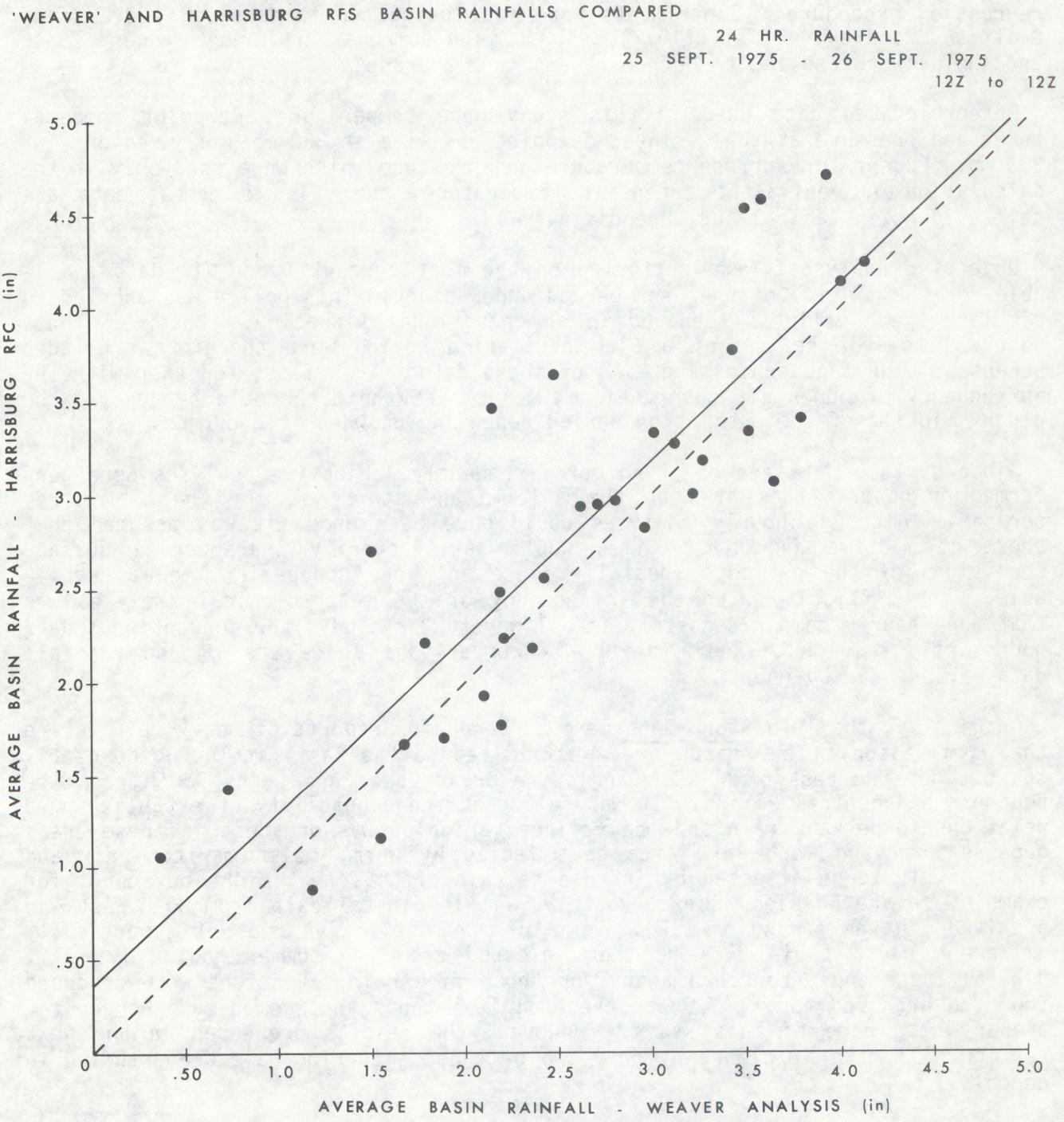

Figure 1 Comparison of average basin rainfall over 24 hr by the RFC and Weaver methods, 1200 GMT to 1200 GMT, 25 to 26 September 1975. Solid line is the line of regression RFC data on Weaver data; dashed line shows the ideal one-to-one relationship.

clouds with average IR temperatures less than an assigned threshold were presumed to produce rain, and only those cloud locations are considered in the regression procedure. Experiments were made using two thresholds, -20°C after Griffith, Woodley, et. al. (1978) and 0°C in a somewhat arbitrary manner. These thresholds were applied to both 6-hr and 1-hr averages.

Meteorological data used in this study were temperature, dewpoint temperature, and pressure at the surface; dewpoint and wind at 850 mb; and wind only at 200 mb. Except for surface temperature and pressure which were used only in the calculation of equivalent potential temperature, the roles of these data are self-evident in table 1 and appendix A.

Objective analyses[3] were performed on the most current upper-air data available for the midtime of the 6-hr period under study. This policy was adopted to simulate the timeliness required in an operational situation. Upper air data observed toward the end of a 6-hr estimation period were therefore precluded because of the long processing time of these data. This fact, together with the infrequency of upper air observations, meant that the data could be up to 12 hr old by midtime of the estimation period depending on when it occurred.

Since surface data are observed more frequently, objective analyses were performed on observations at both the midtime and start time of the 6-hr study periods. Although hourly analyses could have been used, it was assumed that those at midtime and start times would satisfactorily characterize surface conditions of the period, especially since only one upper-air time was available. One difficulty with the infrequency of the meteorological analyses was that when hourly comparisons to rainfall were under study, the conventional data necessarily remained fixed for all six comparisons while the IR and rainfall data varied hour by hour.

Originally, the 1975 Storm Data were screened for reports of heavy rain during the warm season. The search area was limited to the East (including Connecticut but not the rest of New England), the Great Lakes area, the South, and the southern and central Plains. It was felt that the probability of establishing a relationship between rain and the various variables was greatest in these areas because they are most likely to be affected by warm, moist maritime air and least likely to be affected by intense terrain effects that might be found, for example, in the Rockies. Unfortunately, little digital data from GOES East was archived[4] in the spring of 1975. Five of the most active and yet synoptically different days (table 2) were then selected from the summer and early fall. Digital tapes and enhanced imagery for those five rain situations were produced from the archived tape[5]. It was these digital tapes that comprised the geostationary data base of this study. However, the results presented in the next section will make it clear why only two of these situation have been studied in depth.

- - - - - - - - -

[3]Analyses were performed using the objective method of Albert Thomasell, NOAA/NESS, Earth Satellite Laboratory, Atmospheric Sciences Branch.

[4]For many years NASA funded and archived a NESS recording of stretched GOES data. Only one satellite output, GOES East or GOES West, was recorded at any given time.

[5]These products were produced by the Field Services Division of NESS replaying the archive tapes through the operational system into a sectorizer and then into a photographic imaging device.

Table 2 -- Rainfall situations selected

DATE (1975)	TIME RANGE (GMT)	LOCATION
9-10 July	1500-0200	Delaware, Maryland, Pennsylvania, New York
19-20 July	1800-0600	Illinois, Ohio, Kentucky, Tennessee, Indiana
25-26 August	1900-0600	Missouri, Illinois, Arkansas
5-6 September	1230-0300	Ohio, West Virginia, Pennsylvania
25-26 September	1800-1700	Pennsylvania, Maryland, Virginia, West Virginia, Delaware, New York, New Jersey

4. RESULTS

Statistical results of the two situations are presented in this section. Figures 2 and 3 show the locations involved in each. In the first, remnants of Hurricane Eloise affected the East causing heavy rains from Virginia northward during 25 and 26 September 1975. The second, during the night of 25 August 1975, was an entirely different meteorological situation; it was an intense thunderstorm system which produced up to 3 in of rain in a few hours over central Missouri.

Remnants of Hurricane Eloise

This persistent and slow moving tropical system caused heavy rains of up to 10 in and more to fall over central portions of Pennsylvania, Maryland and Virginia during the 4-day period, 22 to 26 September. Some of the heaviest rain fell during the last 24 hr up to 7 a.m. on the 26th. Westminister, Maryland, for instance, received more than 7 in. From these last hours, two adjacent areas were chosen for study in each of two 6-hr time periods. The areas were centered in Pennsylvania and Virginia (figure 2) and will be hereafter referred to in that manner, even though the Virginia area includes portions of Maryland and West Virginia. These cases were ideal for study because of the large effect on riverflow. Pennsylvania, in particular, is a good study area because of the presence of a major river system, the Susquehanna River, and of the heavy density of the hourly network (figure 4 and appendix B). Rain gages beyond these bounds were also used to avoid boundary problems.

Despite the heavy rain, images representative of each period (figure 2) show that cloud tops were not unusually high for convection. The coldest clouds were rarely less than $-55^{o}C$ and more often between $-45^{o}C$ and $-55^{o}C$. Temperatures in that range indicate cloud heights were no more than 35,000 to 40,000 ft. That these ordinary appearing clouds of residual tropical disturbances can have such a profound effect on rainfall and riverflow, make it important to determine whether the rainfall can be estimated from satellite data.

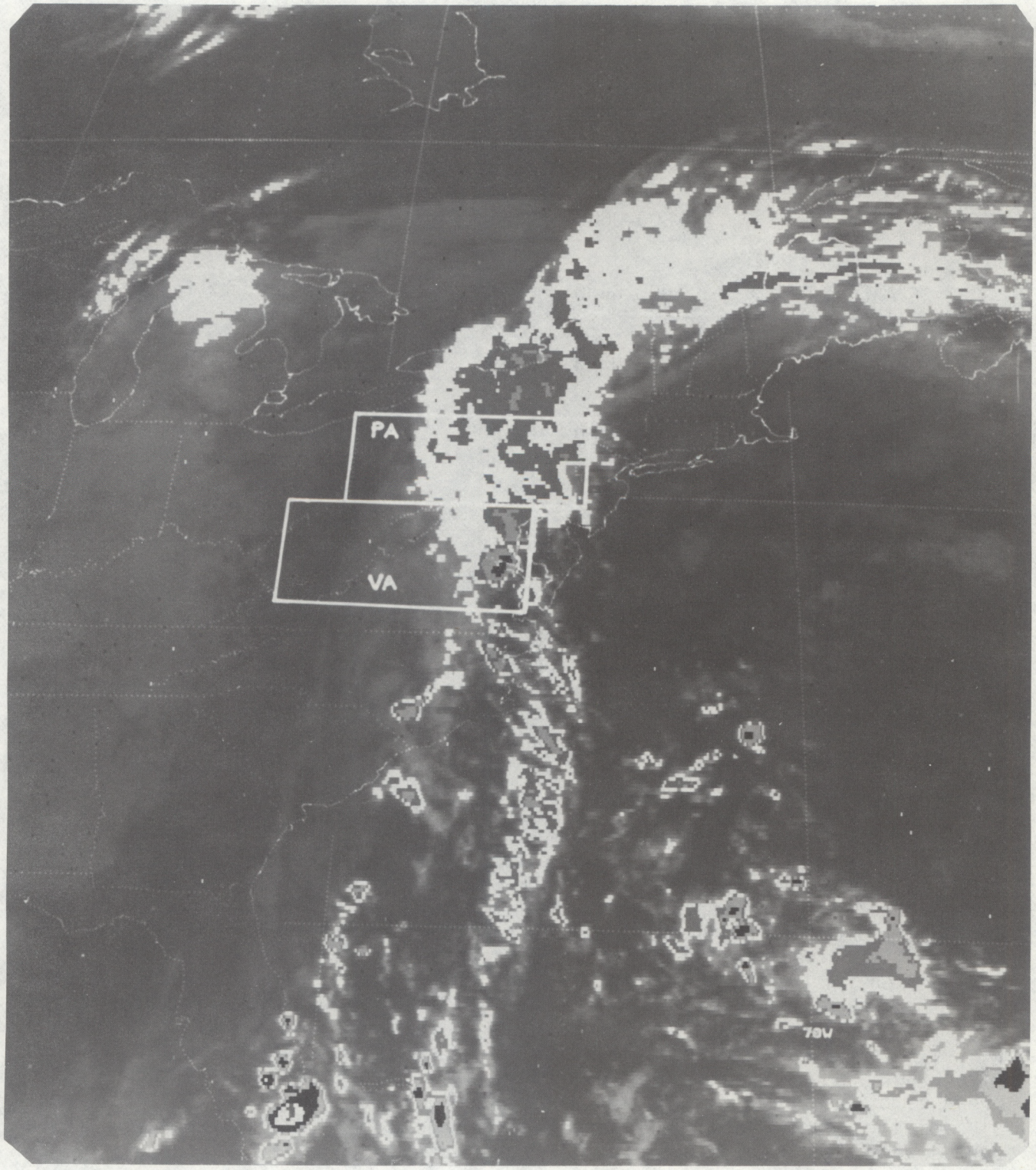

Figure 2a Enhanced IR image at 2100 GMT 25 September 1975. One of six images used during the 6-hr rainfall period 1700-2300 GMT. White represents a blackbody temperature range of -20^{o} to -35^{o} C; dark gray, -35^{o} to -45^{o} C; light gray -45^{o} to -55^{o} C; black, -55^{o} to -65^{o} C.

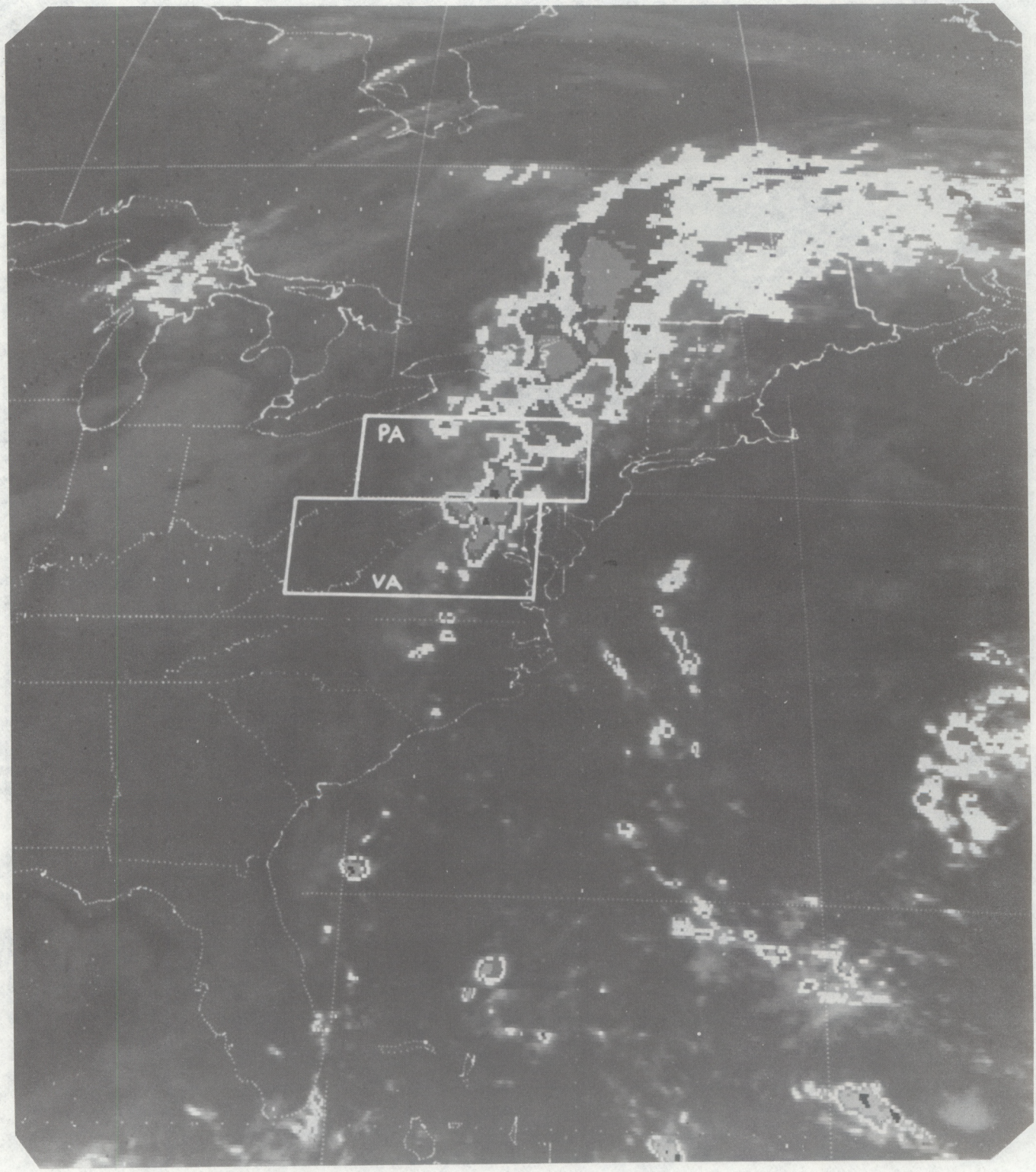

Figure 2b Enhanced IR image at 0800 GMT 26 September 1975. One of six images used during the rainfall period 0500-1100 GMT.

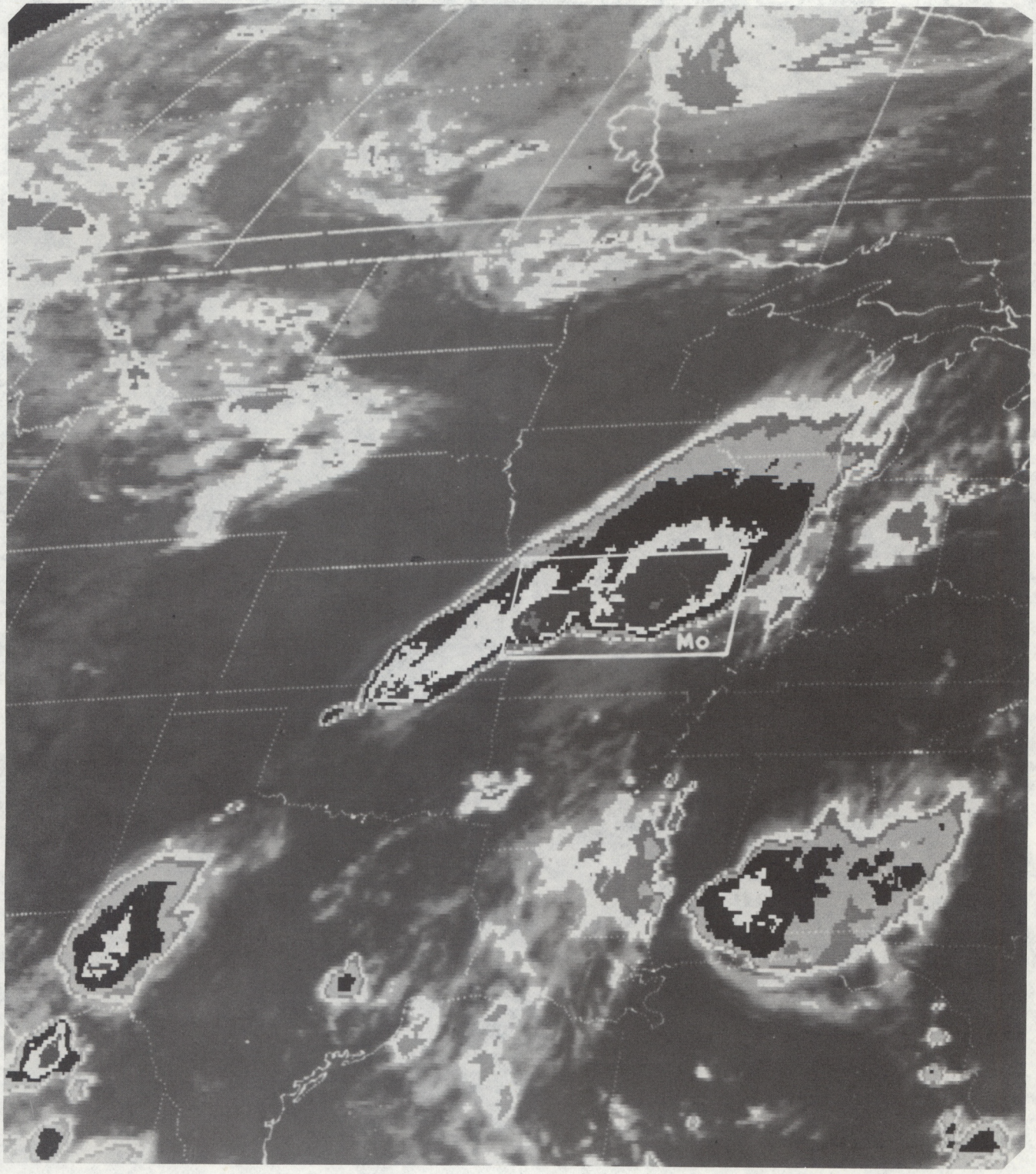

Figure 3 Enhanced IR image at 0230 GMT 26 August 1975. One of six images used during the 6-hr rainfall period 2200 GMT 25 August- 0400 GMT 26 August. Enhancement levels through the first level of black are the same as in figure 2. Second level of white is -65^{o} to -70^{o}C; second level of dark gray, -70^{o} to -75^{o}C; second level of light gray, -75^{o} to -80^{o} C.

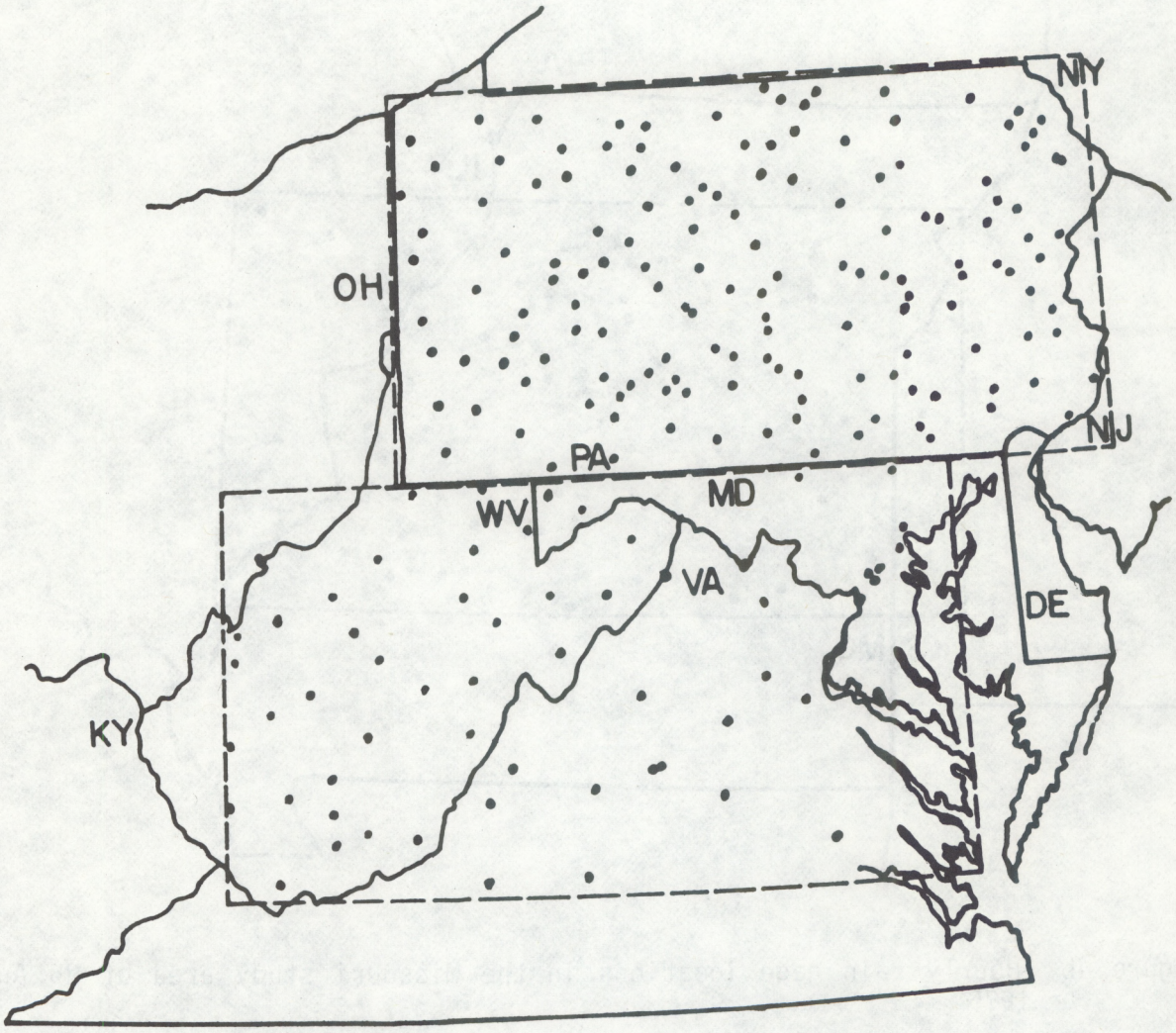

Figure 4a Hourly rain gage networks in the Pennsylvania and Virginia study areas of 25 and 26 September 1975.

a. Statistical results

First, the Pennsylvania case, from 18 - 23 GMT on the 25th (figure 2a), was examined using the threshold IR temperature of -20°C. From the first column in table 3a, it can be seen that a very large percentage of variance of 6-hr rainfall is explained by the variables selected. Variables involving IR temperature played the largest role; the cloud-top temperature gradient along the 850 to 500 mb shear (variable 8) and the IR temperature (variable 2) were the first two variables selected and together correlated at 0.73 with the 6-hour rainfall. Added selections of dewpoint gradients along the 200 mb wind direction (variable 18) and the cloud-top temperature along the 850 mb wind (variable 7) increased

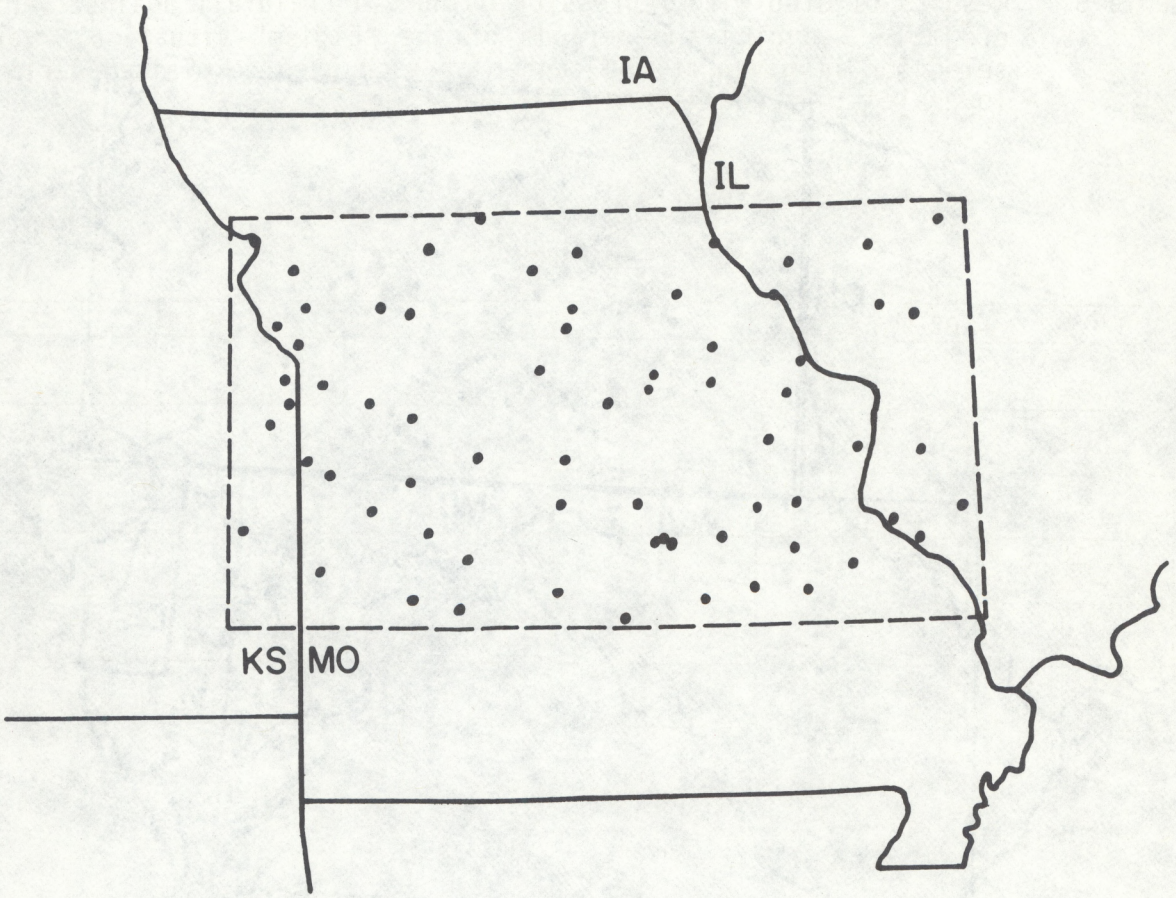

Figure 4b Hourly rain gage locations in the Missouri study area of 25 August 1975.

the explained variance by only 10 percent or increased the correlation to 0.79; nevertheless, models including those variables showed significant statistical improvement in variance over the model using only the first two selected variables.

Addition of the fifth variable (variable 27) offered no significant improvement over the four-variable model. To so signify, the fifth box (step) is shaded in table 3. For future reference, all boxes shaded in tables 3, 4, 6, 9, 11, and 12 represent variables which fail, at the 1 percent confidence level of the F standard statistical test, to produce variances significantly improved over preceeding models composed of fewer variables.

Table 3 Results of step wise regression using 6-hr rainfall against variables of Table 1 during two periods of the "Eloise" situation. Variable selection is given at top center of each step; explained variance at lower left; standard error at lower right.

a

25 SEPTEMBER 1975 18 - 23 GMT

	-20° Threshold			0° Threshold		
	PA	VA	PA & VA	PA	VA	PA & VA
STEP	N = 111	N = 65	N = 176	N = 122	N = 99	N = 221
1	8 40.3 .27	17 57.4 .24	11 30.6 .29	3 31.1 .30	2 64.0 .22	2 42.7 .28
2	2 52.9 .24	22 74.5 .18	2 56.2 .23	2 42.9 .27	9 73.8 .19	11 63.5 .22
3	18 59.2 .22	11 78.5 .17	23 59.2 .22	9 54.1 .24	4 75.7 .18	18 65.5 .21
4	7 62.7 .21	27 79.4 .16	18 62.2 .22	18 57.3 .23	12 77.4 .17	26 66.7 .21
5	27 64.3 .21	2 80.3 .16	14 64.3 .21	3 63.1 .22	22 80.2 .16	4 68.0 .21

b

26 SEPTEMBER 1975 06 - 11 GMT

	-20° Threshold			0° Threshold		
	PA	VA	PA & VA	PA	VA	PA & VA
STEP	N = 74	N = 40	N = 114	N = 111	N = 68	N = 179
1	22 44.7 .49	20 50.4 .26	2 29.2 .49	2 53.5 .45	2 47.4 .28	2 49.5 .40
2	8 51.5 .46	22 58.9 .23	8 49.0 .41	11 79.8 .30	17 54.6 .26	11 64.2 .34
3	2 58.2 .43	9 60.8 .23	26 51.1 .40	25 82.6 .27	4 58.6 .25	26 67.4 .32
4	22 63.8 .40	3 65.0 .22	7 54.4 .39	4 83.8 .26	12 62.0 .24	4 69.4 .31
5	26 68.0 .38	9 66.3 .21	18 55.9 .38	2 84.3 .26	3 63.6 .23	25 69.9 .31

Although these results showed promise, they needed testing for stability and repetition at other times and places. To examine these points, the adjacent area of Virginia was studied for the same time period (figure 2a) and the same Pennsylvania and Virginia areas were studied for the later time, 05 - 11 GMT on 26 September (figure 2b) - a time period still dominated by the same meteorological situation.

Column 1 of table 3b indicates that, although the variables 8 and 2 were repeated on the second day in Pennsylvania, both gave way to variable 22 (laplacian of surface dewpoint at the start of period) as the dominant variable. Inspection of table 3 reveals similar, albeit more extreme, variability in the Virginia area from the first day to the second. Also, the Virginia selections bore little resemblance to those in Pennsylvania.

Explained variances also fluctuated among the four cases. As shown by the unshaded boxes in table 3, the number of variables explaining significant amounts of variance also fluctuated from five to two among these four cases.

When Pennsylvania and Virginia areas were combined for each day, the explained variances decreased and some selections changed yet again. But, variables 2, 8, and 11 still showed up as important ones. Variables 8 and 11 are quite similar in that 11 is simply the product of variables 8 and 2, so that all three involve IR cloud-top temperature or its gradient along the tropospheric shear direction.

By setting a higher threshold of cloud-top temperature, i.e., $0^{o}C$ for discriminating rain clouds from no-rain clouds, new data sets were generated for the same areas and times just discussed. These data sets were different in two respects from those obtained by using a $-20^{o}C$ threshold. First, the sample sizes were larger because of the additional warm-cloud samples, and second, the IR temperatures of the previously selected samples were prone to revision upward (warmer) because of the potential for including higher values in the averages. Therefore, values of all variables involving IR temperatures were subject to change from those using a $-20^{o}C$ threshold. The variables selected and the associated statistics derived by using the $0^{o}C$ threshold data are shown in the right half of tables 3a and 3b.

Use of the $0^{o}C$ data set caused the variable selections to change and the order of selection to be altered from area to area and day to day. Nevertheless, variable 2, the IR temperature, was again a frequent selection just as it was for the lower threshold. Also, when Pennsylvania and Virginia data were combined for each day, variables 2 and 11 emerged again as prime selections. Variables 26 and 18, the terrain height and surface dewpoint gradient along the 200 mb wind, were two secondary selections which had also been chosen when using the lower threshold.

Examination of the intercorrelations between variables in each of the combined cases above demonstrated that, indeed, variables 2 and 11 were the best selections since they were correlated best with rainfall for the least correlation to each other. Variable 18, although generally better correlated with rainfall than variable 26, tended to be too well correlated with both 2 and 11. Because of these facts, all data from both areas for both days were combined, and regression equations for each threshold were derived using variables 2, 11, and 26. Table 4 shows a summary of these statistical results.

When the data sets were combined, variance reductions became generally lower as before. The three-term model using the $-20^{o}C$ threshold failed the signifi-

cance test and that using the 0°C threshold barely passed, while the standard error improved by only 0.01 in. Therefore, the most promising relationships to rainfall appeared to stem from variables 2 and 11 only.

Table 4 -- Results of the stepwise regression using 6-hr rainfall for all cases combined in the "Eloise" situation - 1700-2300 GMT 25 September 1975 and 0500-1100 GMT 26 September 1975.

	-20°C THRESHOLD		0°C THRESHOLD	
STEP	PA & VA N = 290		PA & VA N = 400	
1	2	18.9 .43	2	35.8 .38
2	11	37.8 .38	11	49.6 .34
3	26	38.9 .38	26	51.4 .33

Table 5 shows that three-quarters of the additional samples in the "warm" model (0°C threshold) over those in the "cold" model (-20°C threshold) were associated with rain of 0.25 in or less, and all were an inch or less. The difference between models was then largely accounted for by these low-rainfall samples. Other factors, as noted before, are that sample locations common to both models may have different IR temperatures and thus different IR gradients as well. Since these last two factors are critical to the value of the two variables common to both final models, then they can cause some differences between the models too.

Table 5 -- Frequency distribution of rain and no-rain samples (as determined by each of two thresholds) into classes of observed rainfall, -1700-2300 GMT 25 September and 0500-1100 GMT 26 September.

	6-HR OBSERVED RAINFALL											
RAIN	0	.01-.25	.26-.50	.51-.75	.76-1.00	1.01-1.25	1.26-1.50	1.51-1.75	1.76-2.00	2.01-2.25	2.26-2.50	2.51-2.75
SAMPLES ≤ -20°	0	65	64	60	43	24	16	11	3	2	1	1
SAMPLES ≤0°	13	136	82	65	46	24	16	11	3	2	1	1
DIFFERENCE	13	71	18	5	3	--	--	--	--	--	--	--
NO-RAIN												
SAMPLES >-20°	159	111	20	8	4	--	--	--	--	--	--	--
SAMPLES >0°	146	40	2	3	1	--	--	--	--	--	--	--
DIFFERENCE	-13	-71	-18	-5	-3	--	--	--	--	--	--	--

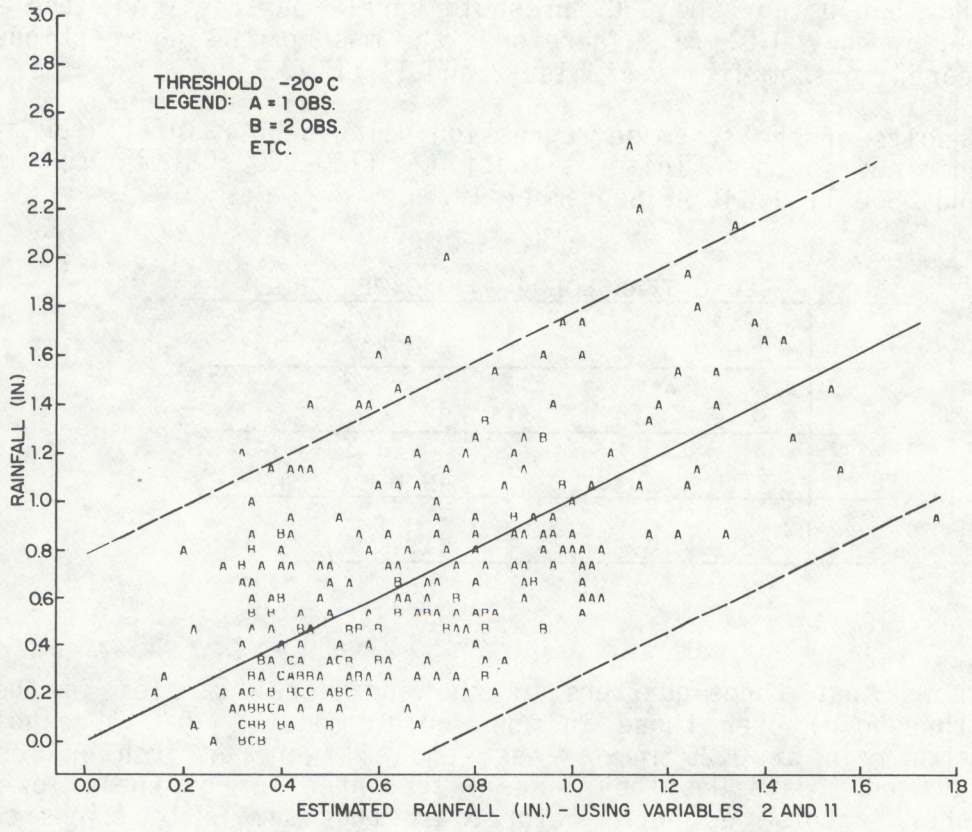

Figure 5a Scatter diagram comparing observed 6-hr rainfall with the regression estimate obtained using dependent data of 25 and 26 September 1975. All four cases of "Eloise" used in the regression development are included. Only variables 2 and 11 are involved and the -20°C-threshold equation is used. Solid line represents the ideal relationship; dashed lines represent scatter extremes equal to twice the standard error.

Scatter resulting from combining these two final variables against observed rainfall was appreciable at either threshold (figures 5a and 6a). Residuals of observed rainfall plotted against these two-term models derived from either threshold (figures 5b and 6b) showed many large residuals and much pattern. Around 4 percent of the residuals lay beyond twice the standard error, and the scatter of residuals increased with increasing amounts of model rainfall. Both of these characteristics were also found when using the IR temperature alone (figures 7 and 8). Such evidence suggests that the data were neither normally distributed nor random. Therefore, the models need improvement at best and at worst are invalid.

Attempts to eliminate these problems by a transformation of variables, specifically by relating the ratio of rainfall and IR temperature to the inverse IR temperature, failed. Some experimentation (Whitney and Herman, 1981) was made including the squares of variables, but these attempts made little substantial improvement. Moreover, there seemed to be no physical reason to involve squares of variables.

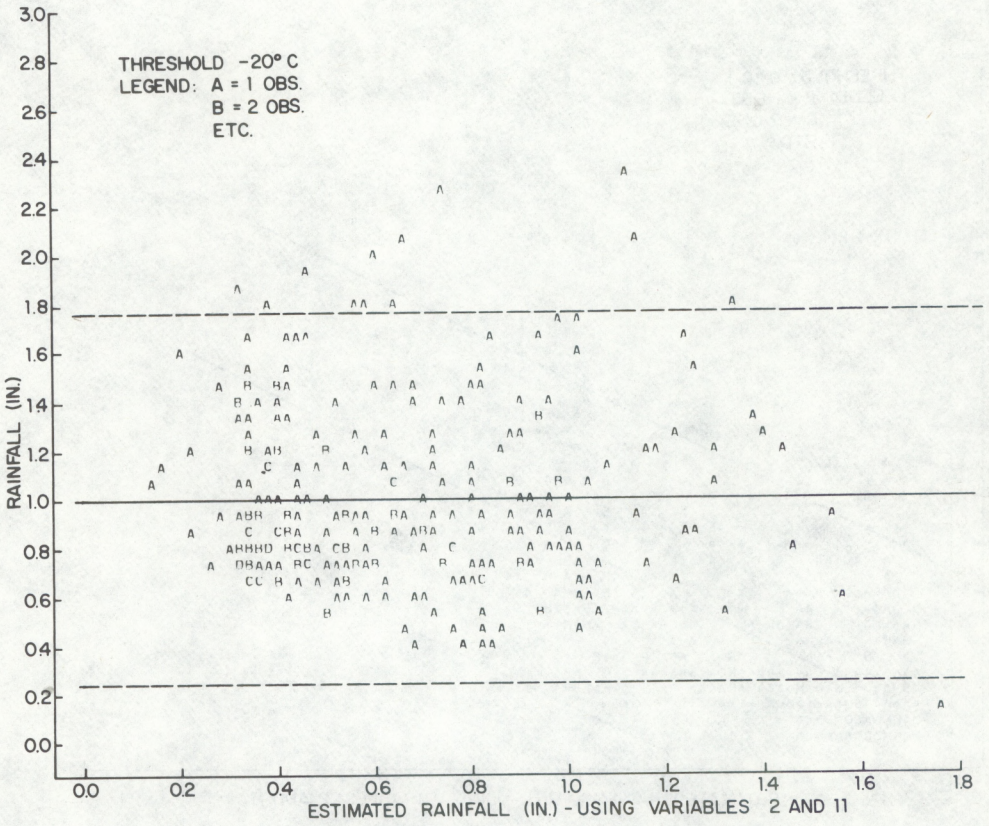

Figure 5b Residual vs estimated rainfall for the same data set as in figure 5a. Dashed lines represent standardized residuals of ± 2.

Despite these somewhat negative results, testing of the final models with dependent data seemed a chance to provide some additional measure of their practical worth. Credibility of any model depends upon its ability to reproduce the rainfall of individual cases from among those used to generate the model. If the rainfall can be reproduced to useful accuracy, the model has potential and should be tested further against independent data; if not, the model is discredited since there is no reason to suspect that it should behave better using independent data.

Tests of the 0^{o}-threshold model using each of the four Hurricane Eloise cases are presented in figures 8 through 11. The first test, using the Pennsylvania case of 26 September, was the one test that should have most readily verified the "warm" (0^{o}C) model. This model explained more variance than the "cold" (-20^{o}C) model, and the above-cited Pennsylvania case was correlated best with rainfall. Also, the first two variables selected were the same as in the final model of all cases; moreover, these same Pennsylvania data comprised more than one-fourth of the data used in developing the final model. Figure 8 shows the estimated rainfall, the observed rainfall, and difference between the two. Although the areas of predicted and actual rainfall agreed well, the amounts, particularly those associated with heaviest rain, showed large error. Tests of this model against the remaining three cases gave equally disappointing results (figures 9 through 11). The same was true for tests of the "cold" (-20^{o}C) model against each case (not shown).

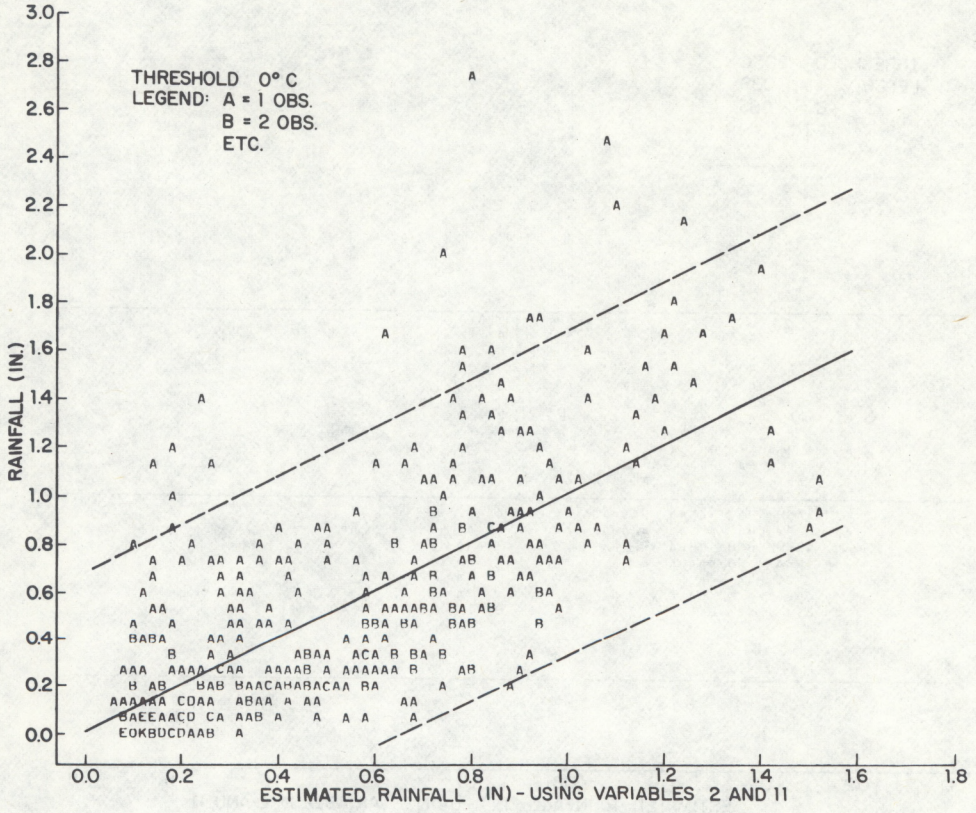

Figure 6a Same as figure 5a except that the 0^{0} threshold is used.

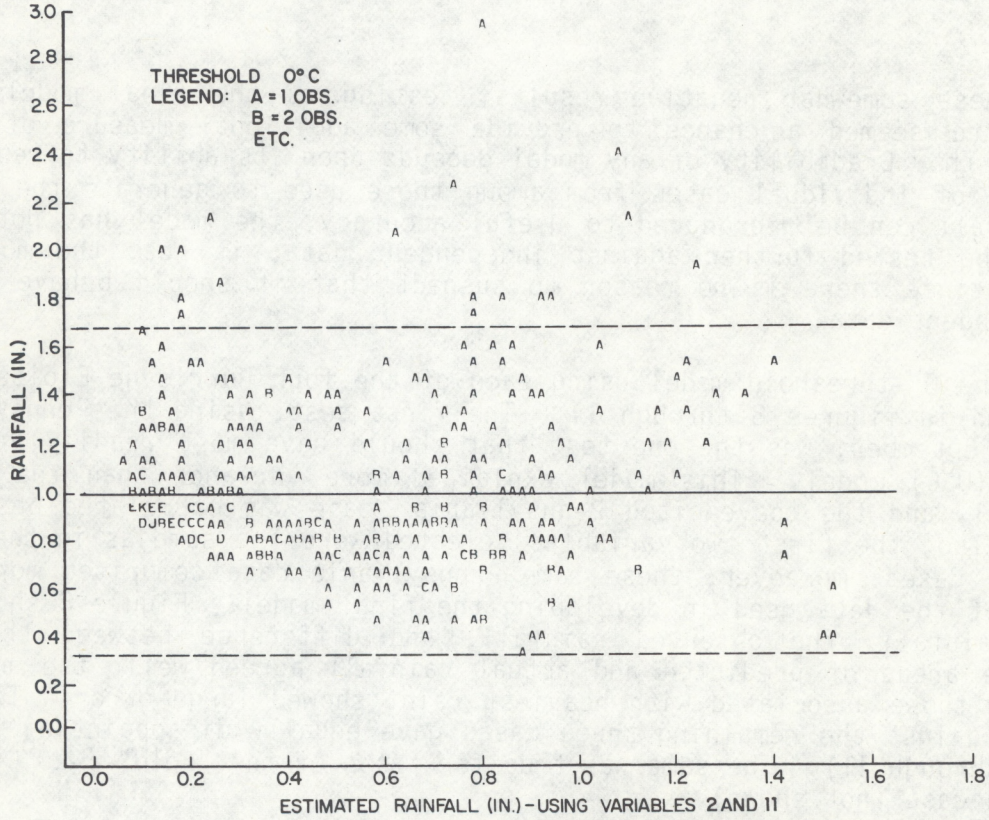

Figure 6b Same as figure 5b except that the 0^{0} threshold is used.

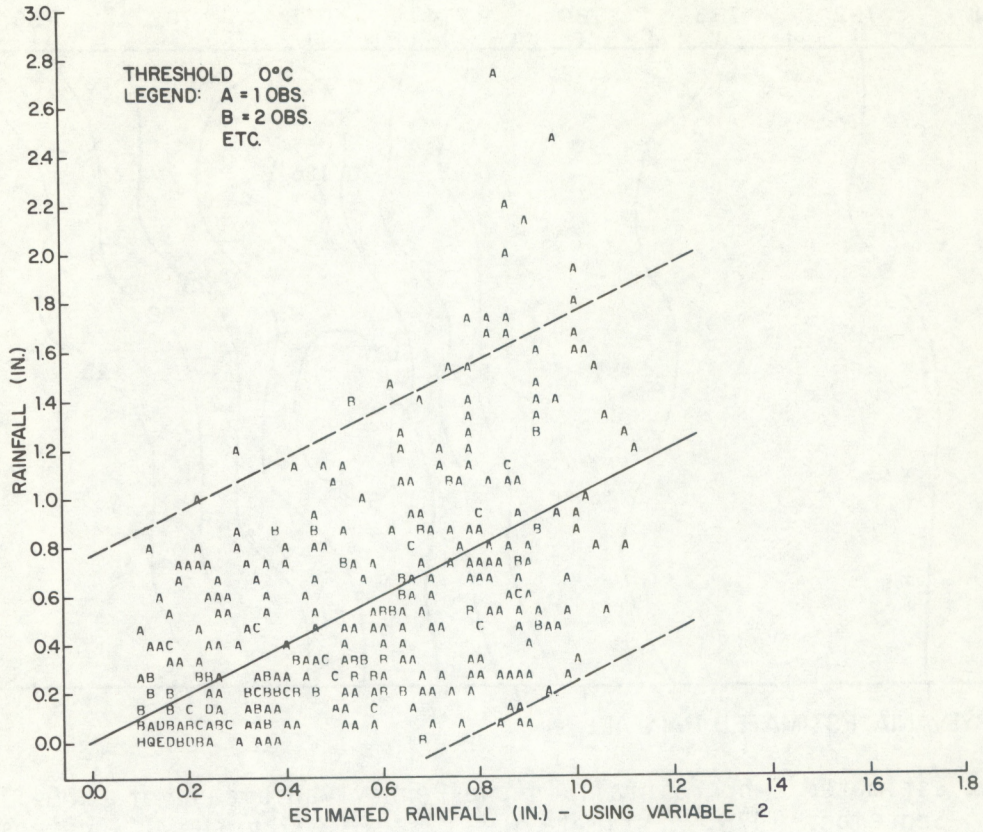

Figure 7 Same as figure 6a except that only variable 2 is involved.

Since the crude method of averaging IR temperatures over 6-hr affected all IR related variables and perhaps their relation to 6-hr rainfall, an adjunct experiment was run to determine whether hourly values might relate better to hourly rainfall. Although still being areal averages, hourly temperatures require no time averaging and thus may vary greatly from one hourly picture to the next. As a result, rain cloud selections as well as the values of any IR-related variables (2 through 11) may vary hourly. Unfortunately, all other variables necessarily remained fixed in value from hour to hour since they were based on data at fixed times. Nevertheless, such an examination presented an opportunity to see how the IR variables would behave on an hourly basis.

Statistical results of these hourly comparisons on September 26 are outlined in table 6. Results are highly variable from hour to hour and case to case, particularly with regard to the variables selected and the associated reductions in variance. Surprisingly, the IR variables are not often among the first one or two selections.

Small sample sizes could well be part of the problem here. Also, chance colocations between patterns of fixed variables with patterns of changing hourly rainfall could lead to unrealistically good correlations with first one variable and then another. Such chance relationships could preempt the selection of

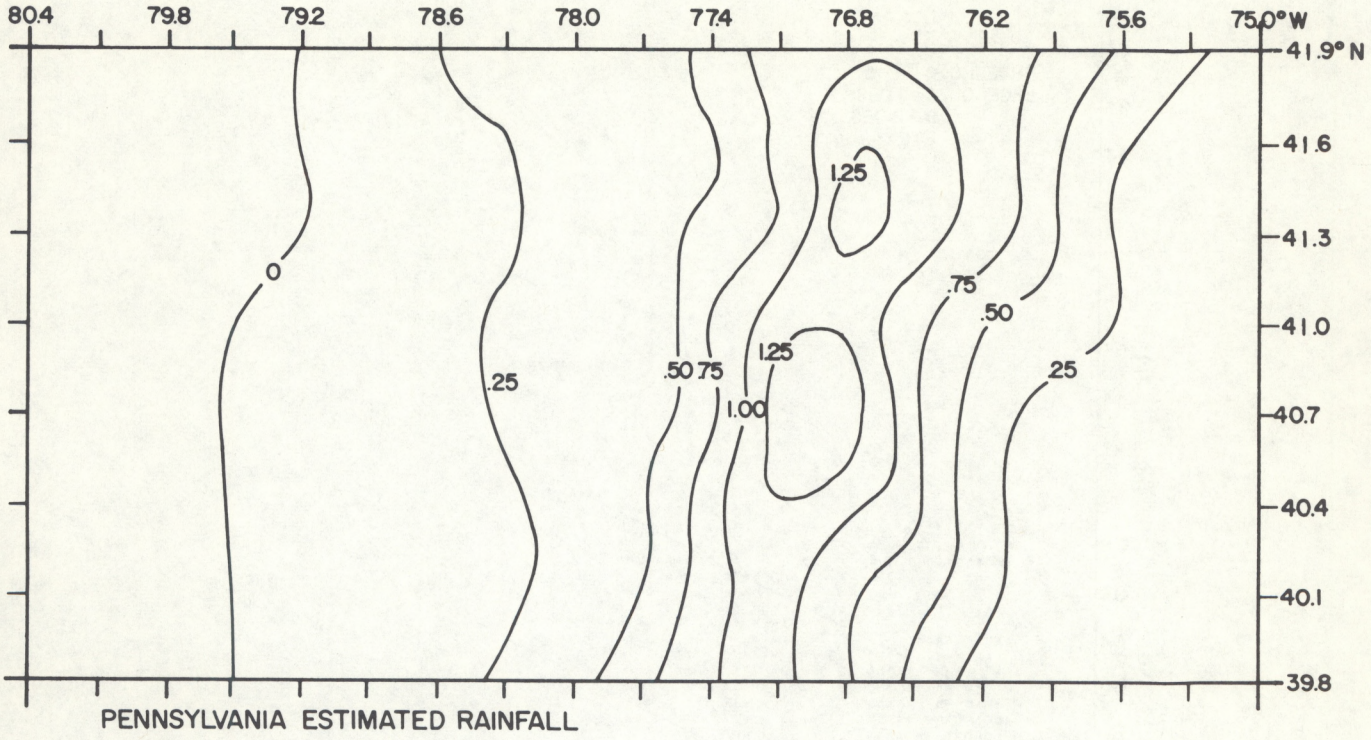

Figure 8a Estimated 6-hr rainfall in the Pennsylvania case of 0500-1100 GMT, 26 September 1975. Estimate was calculated by the $0^{o}C$ regression equation derived from four "Eloise" cases and substituting the dependent data of this one case. Only variables 2 and 11 are involved.

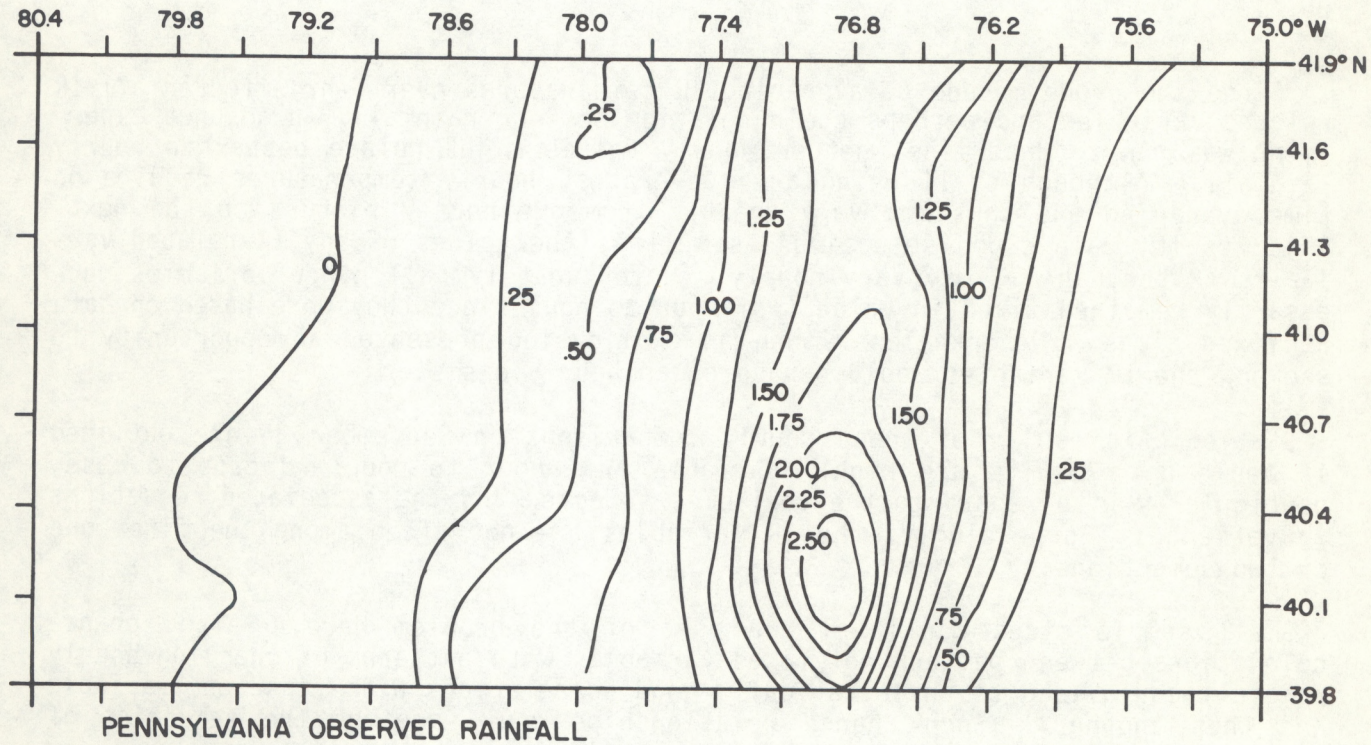

Figure 8b Observed rainfall for the same period.

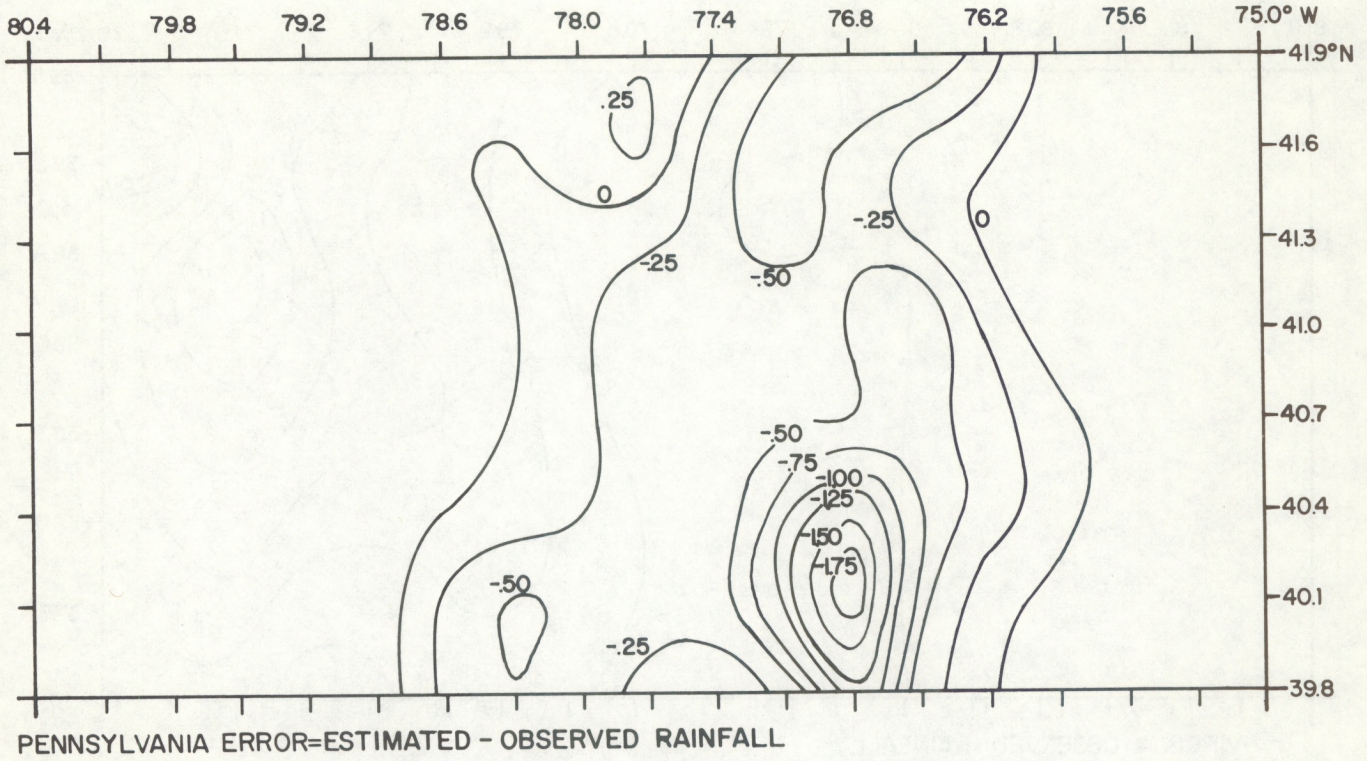

Figure 8c Difference of 8a and 8b.

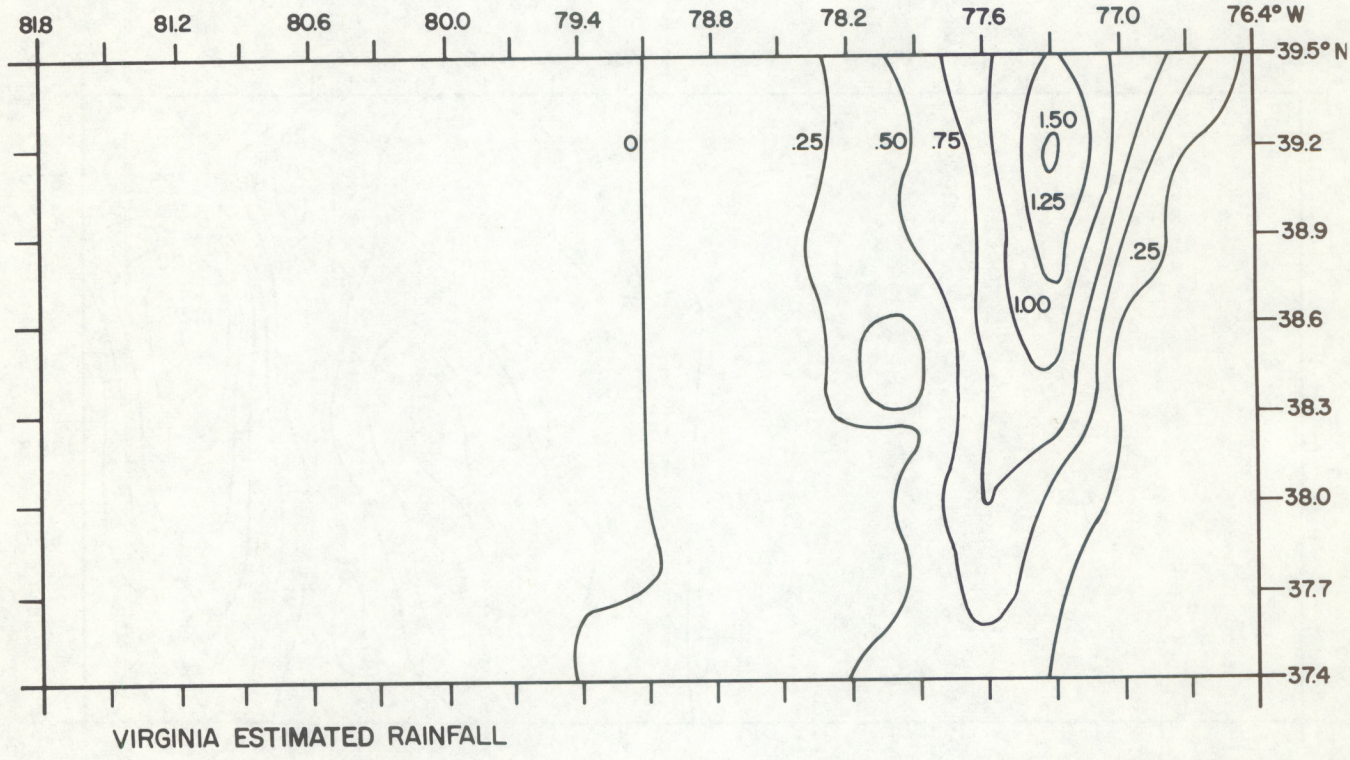

Figure 9a Estimated 6-hr rainfall in the Virginia case of 0500-1100 GMT, 26 September 1975. Otherwise the estimate is made under the same conditions as in figure 8a.

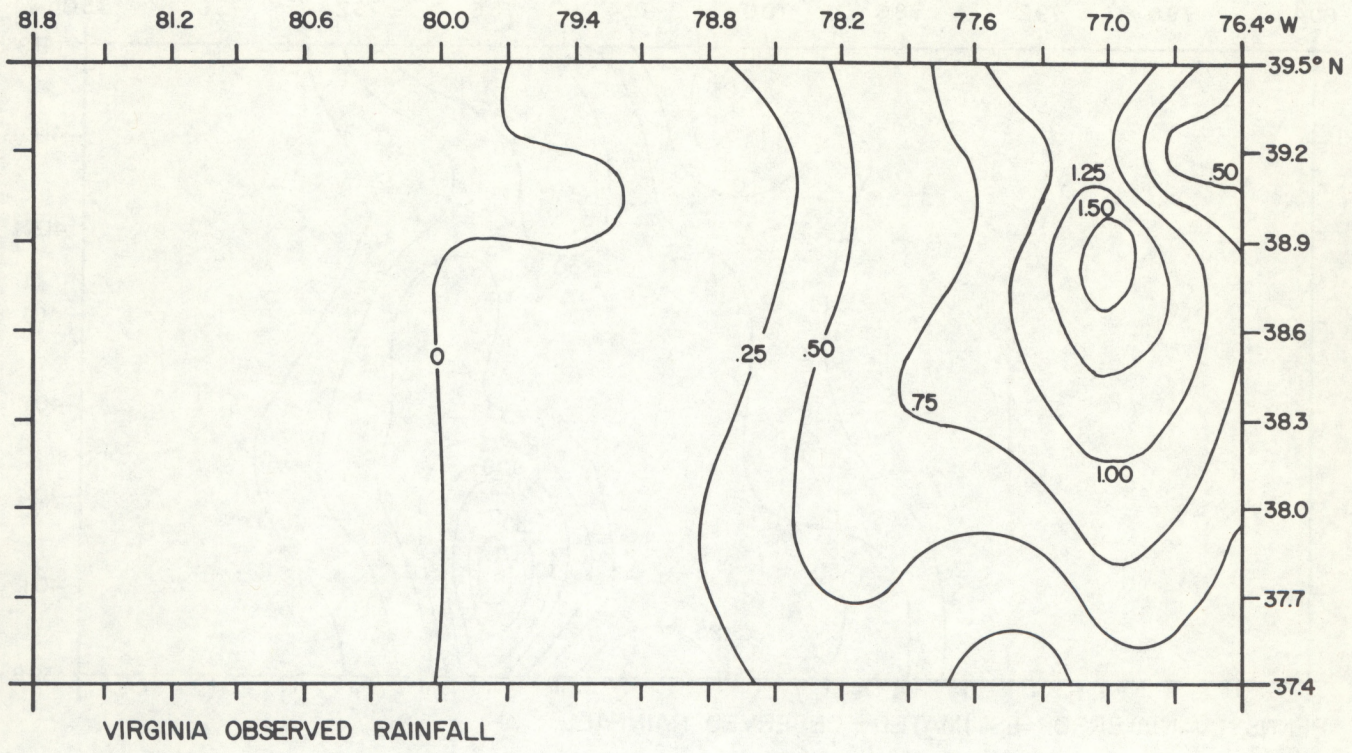

Figure 9b Observed rainfall for the same period.

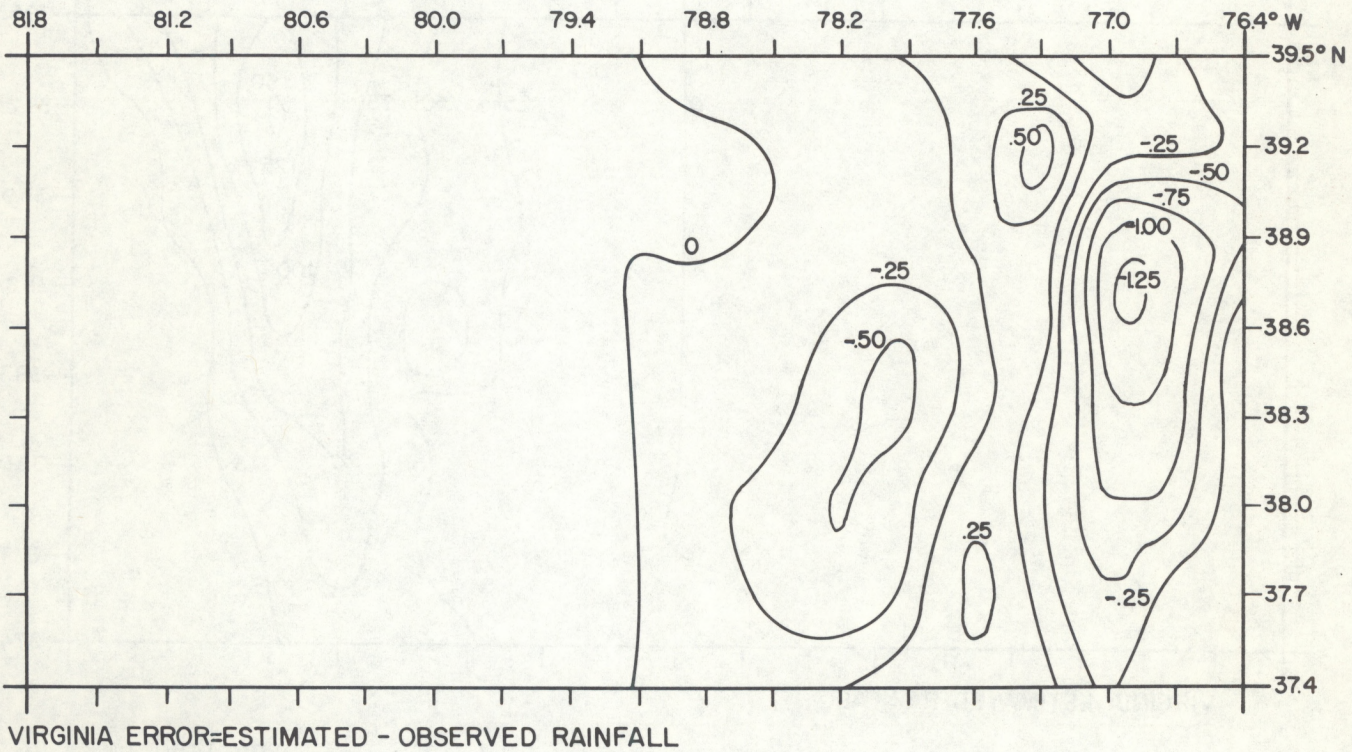

Figure 9c Difference of 9a and 9b.

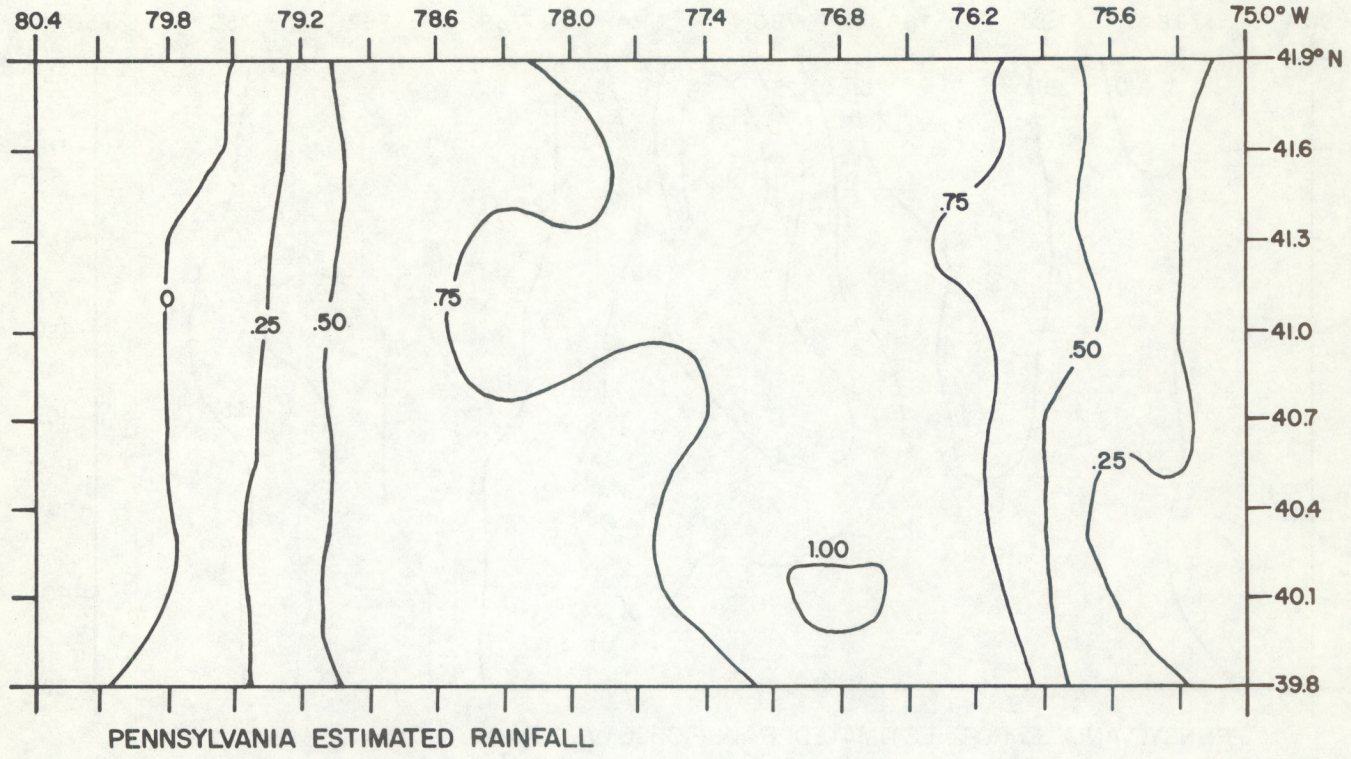

Figure 10a Estimated 6-hr rainfall in the Pennsylvania case of 1700-2300 GMT, 25 September 1975. Otherwise the estimate is made under the same conditions as in figure 8a.

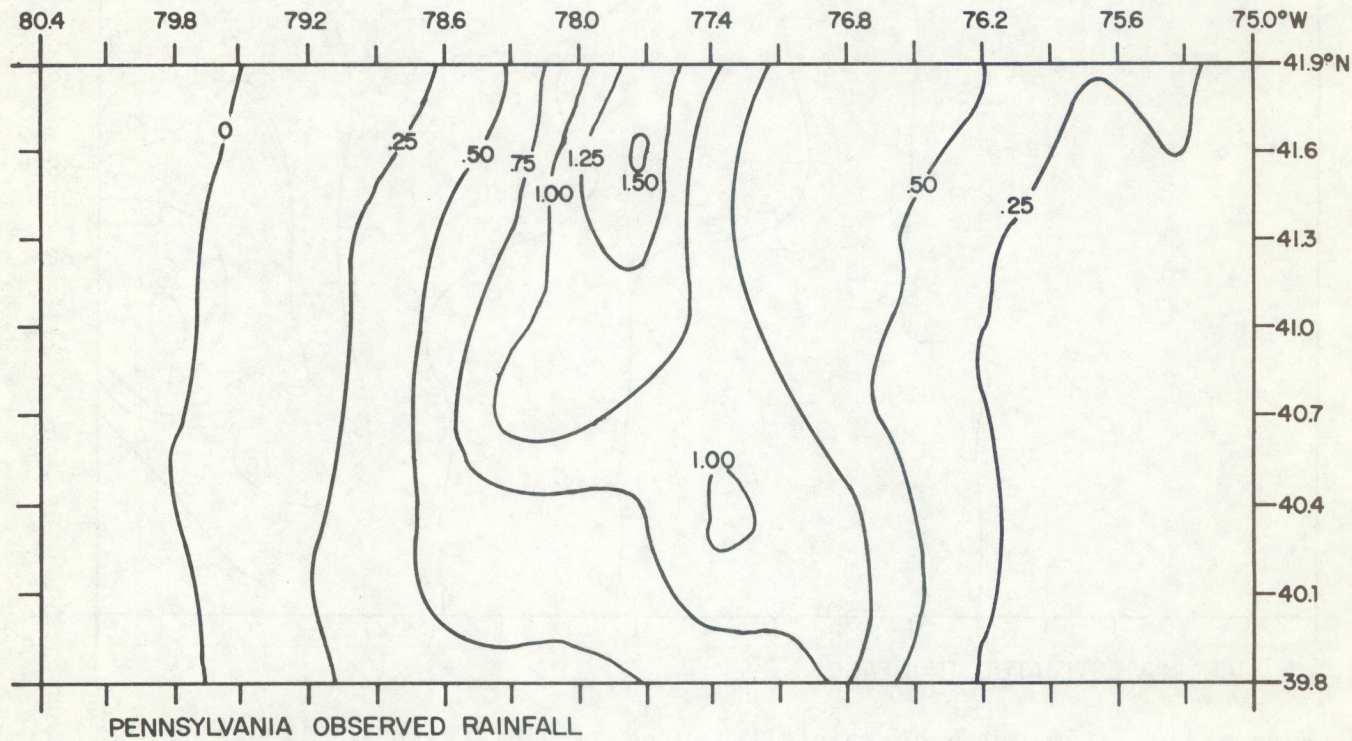

Figure 10b Observed rainfall for the same period.

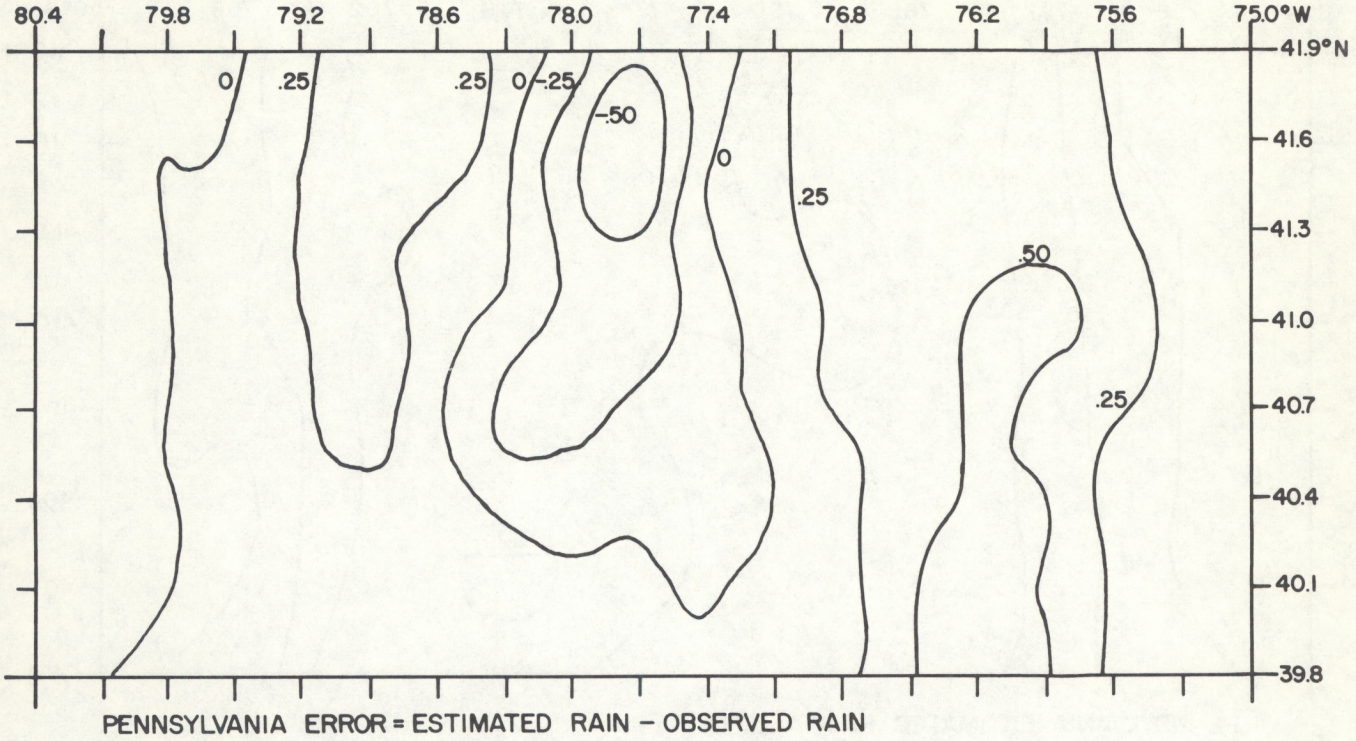

Figure 10c Difference of 10a and 10b.

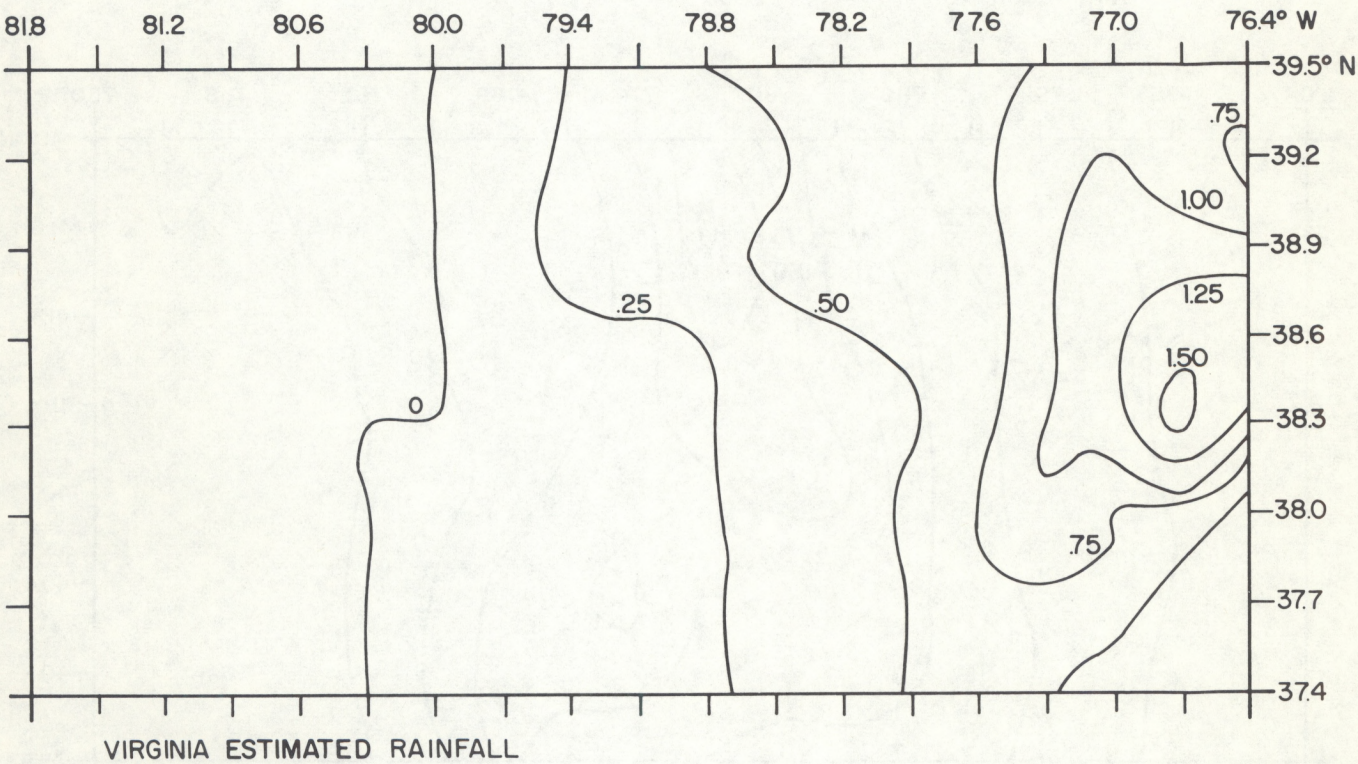

Figure 11a Estimated 6-hr rainfall in the Virginia case of 1700-2300 GMT, 25 September 1975. Otherwise the estimate is made under the same conditions in figure 8a.

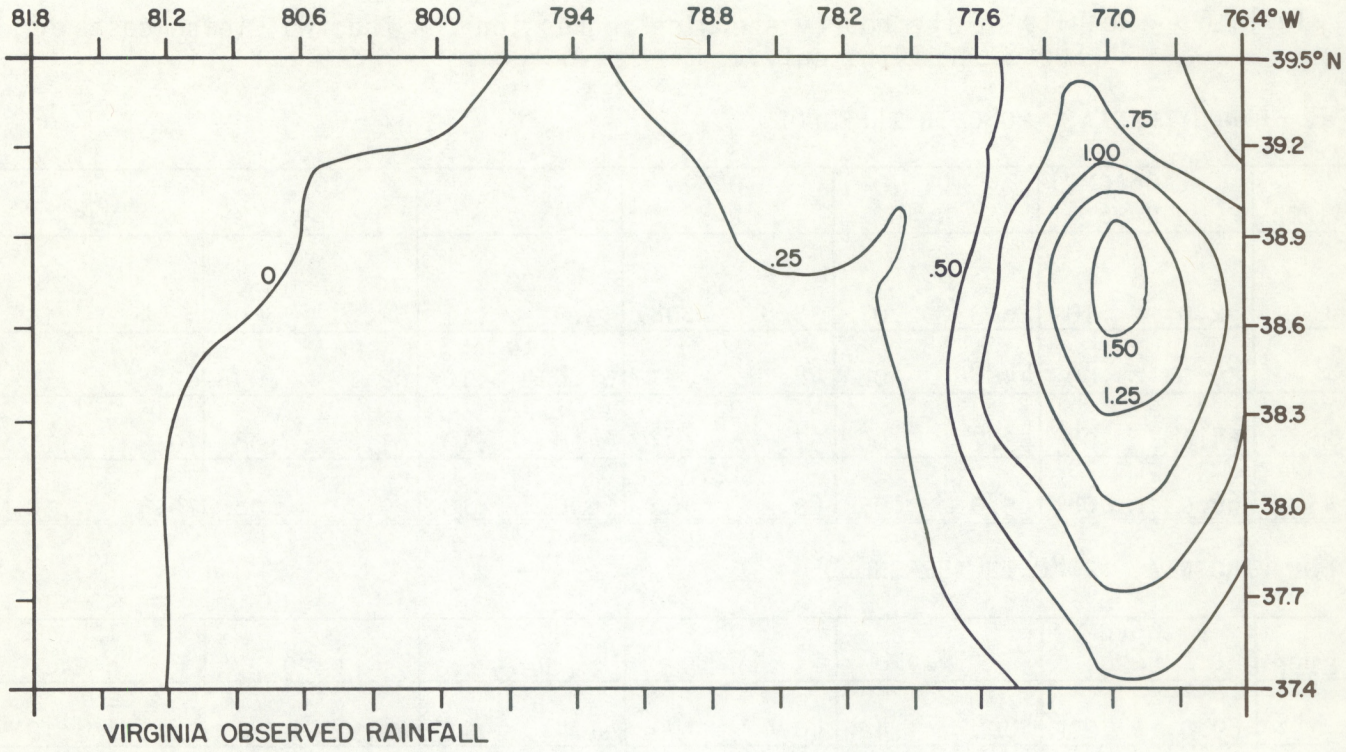

Figure 11b Observed rainfall for the same period.

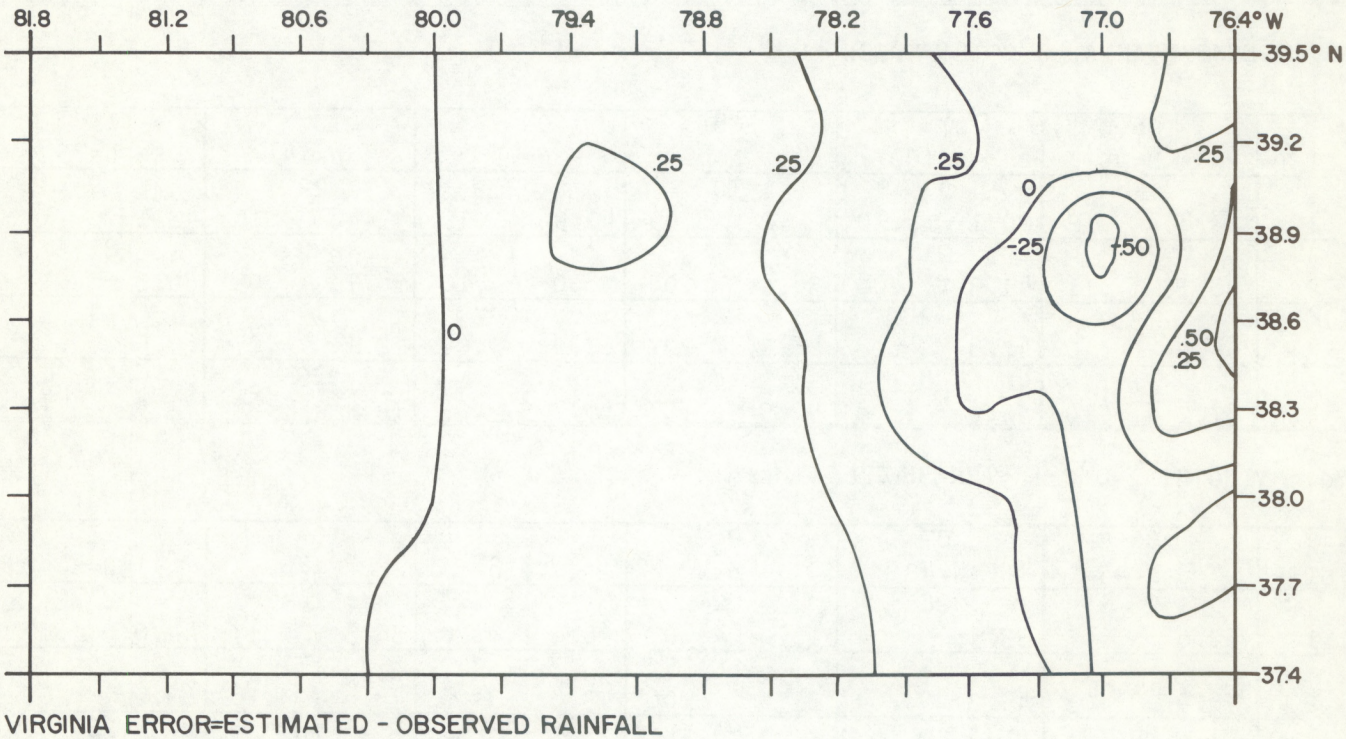

Figure 11c Difference of 11a and 11b.

Table 6 -- Results of the hourly stepwise regression for the two Eloise cases on 26 September 1975, only.

a. PENNSYLVANIA, -20°C IR THRESHOLD

STEP	06(GMT) N=36	07 N=40	08 N=38	09 N=43	10 N=52	11 N=53
1	8 52.0 .10	22 26.3 .07	7 35.8 .08	22 53.5 .11	22 52.6 .10	3 42.4 .15
2	25 59.0 .09	23 44.4 .06	8 48.7 .07	14 61.0 .10	3 62.1 .09	13 63.8 .11
3	23 64.6 .08	3 53.7 .06	22 57.7 .07	2 64.0 .10	14 67.8 .08	21 70.6 .11
4	24 66.9 .08	19 65.0 .05	12 63.2 .06	17 66.6 .10	4 69.5 .08	23 72.4 .10

b. VIRGINIA, -20°C IR THRESHOLD

STEP	06(GMT) N=20	07 N=24	08 N=15	09 N=14	10 N=20	11 N=24
1	23 69.0 .20	26 48.0 .42	2 40.4 .08	26 47.4 .13	12 28.9 .21	20 38.9 .12
2	5 78.3 .17	7 54.6 .39	14 53.2 .07	22 59.4 .11	20 64.5 .15	23 49.8 .11
3	9 79.9 .16	20 59.9 .37	4 60.8 .07	9 65.3 .10	16 74.2 .13	3 57.4 .10
4	16 80.6 .16	19 65.0 .34	21 67.1 .06	27 68.8 .10	20 77.4 .12	26 60.0 .10

c. PENNSYLVANIA, 0°C IR THRESHOLD

STEP	06(GMT) N=95	07 N=100	08 N=89	09 N=75	10 N=74	11 N=75
1	11 23.8 .12	23 20.1 .10	10 22.2 .09	2 41.9 .12	22 47.4 .10	2 43.1 .14
2	26 38.1 .11	21 41.3 .08	17 38.4 .08	11 58.0 .10	3 58.7 .09	21 56.3 .13
3	23 45.5 .10	2 47.8 .08	22 46.0 .07	10 67.0 .09	14 72.1 .07	4 63.5 .11
4	7 47.2 .10	8 52.6 .08	8 52.9 .07	19 69.7 .09	23 74.4 .07	17 71.5 .10

d. VIRGINIA, 0°C IR THRESHOLD

STEP	06(GMT) N=45	07 N=43	08 N=42	09 N=38	10 N=44	11 N=54
1	23 52.6 .03	26 33.3 .04	2 25.0 .07	16 36.6 .10	12 35.3 .17	23 44.0 .12
2	2 56.9 .03	2 49.3 .04	8 33.8 .06	2 43.8 .09	17 43.6 .16	25 63.9 .09
3	20 60.2 .03	6 55.8 .04	4 39.3 .06	7 51.3 .08	16 47.3 .15	22 66.8 .09
4	19 62.1 .03	4 61.6 .03	15 42.4 .06	11 54.4 .08	25 55.8 .14	7 69.5 .09

IR-related variables in any given hour. However, hourly plots of correlation coefficient (figure 12) taken from the most populous case, Pennsylvania on September 26, show highly erratic behavior (using either threshold) by key IR variables as well. Correlation coefficients of other IR variables not shown in figure 12 were also erratic or lowly correlated or both. Similar results (not shown) are true of the Virginia area on that date.

b. Examination of Threshold Levels

All statistical samples in this study were selected on the basis of either of two IR temperature thresholds. These thresholds, were examined to determine just how well they discriminate rain from no rain. Contingency tables 7a and 7b are the results found by applying both thresholds on the combined Pennsylvania and Virginia 6-hr cases of both days. Overall, the $0^{o}C$ threshold best separates the 6-hr averages of IR temperature into rain and no-rain cases. Since only the estimated rain column represents samples used in deriving the statistical regressions already shown, it is especially important to note in table 7a that about 89 percent of all cases of observed rain were correctly assessed and that 97 percent of all cases of estimated rain were verified. Of the 46 rain cases undetected by the $0^{o}C$ threshold, only six were greater than 0.25 in (table 5). By comparison, of the 143 cases undetected by the $-20^{o}C$ threshold (table 7b), 34 were greater than 0.25 in.

The contingency table (table 8a) of hourly decisions between rain and no rain on September 26[6] using the $0^{o}C$ threshold reveals similar though somewhat inferior results to those of the 6-hr decisions on September 25 and 26. It shows that 93 percent of all rain estimates were correct and 76 percent of observed rain was correctly assessed.

Decisions between rain and no rain obtained by applying the $-20^{o}C$ threshold to hourly data were the most inferior of all (table 8b). This result is yet another indication of superiority of the $0^{o}C$ threshold over the $-20^{o}C$ threshold, at least in this particular meteorological situation.

Squall Line in Missouri, 25-26 August, 1975, 22-04 GMT

A squall line affecting much of northern and central Missouri grew and intensified during this period, producing locally heavy rain (up to 3 in). The line was in very warm, moist air just ahead of a cold front approaching from the northwest. These thunderstorms, judging by the cold tops and highly organized thermal pattern of figure 3 reached much greater heights and greater local convective intensity than did convection in the Eloise situation previously discussed. (See figure 2 for comparison.)

The density of the hourly rain-gage network in Missouri study area is depicted in figure 4a. It is the network from which the area-averaged rainfall is derived, although gages beyond these bounds were also used just as in the Pennsylvania and Virginia cases.

---

[6]Data for September 25 was omitted only because the regression results given earlier did not justify the additional effort to include them.

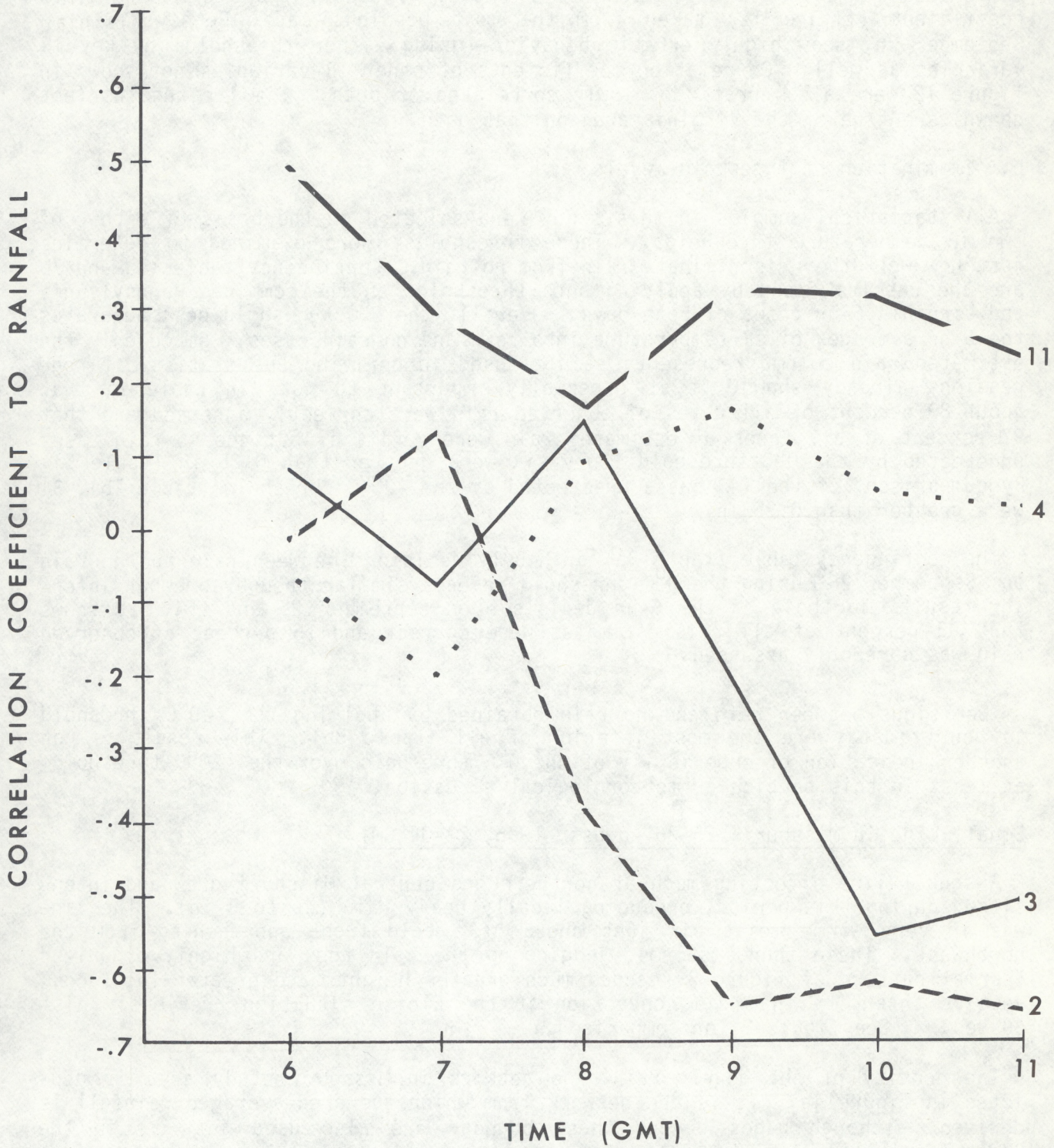

Figure 12 Hourly correlation coefficients of four IR variables to observed rainfall in the Pennsylvania case of 0500-1100 GMT, 26 September 1975. $0^{o}C$ threshold is used.

Table 7 -- Contingency tables of observed vs estimated instances of 6-hr rain (R) and no rain (NR) for combined cases of Pennsylvania and Virginia on 25 and 26 September 1975.

a. $0^{\circ}C$ THRESHOLD

OBSERVED	ESTIMATED R	ESTIMATED NR	TOTALS	OBSERVATIONS CORRECTLY ASSESSED
R	387	46	433	89.3%
NR	13	146	159	91.8%
TOTALS	400	192	592	
EST. COR.	96.8%	76.0%		

b. $-20^{\circ}C$ THRESHOLD

OBSERVED	ESTIMATED R	ESTIMATED NR	TOTALS	OBSERVATIONS CORRECTLY ASSESSED
R	290	143	433	67.0%
NR	0	159	159	100%
TOTALS	290	302	592	
EST. COR.	100%	52.6%		

Table 8 -- Contingency tables of observed vs estimated instances of hourly rain and no rain (NR) in the Pennsylvania and Virginia cases of 26 September 1975 only.

a. $0^{o}C$ THRESHOLD

OBSERVED	ESTIMATED R	ESTIMATED NR	TOTAL	OBSERVATIONS CORRECTLY ASSESSED
R	719	221	940	76%
NR	57	779	836	93%
TOTALS	776	1000	1776	
EST. COR.	93%	78%		

b. $20^{o}C$ THRESHOLD

OBSERVED	ESTIMATED R	ESTIMATED NR	TOTALS	OBSERVATIONS CORRECTLY ASSESSED
R	370	573	943	39%
NR	9	824	833	99%
TOTALS	379	1397	1776	
EST. COR.	98%	59%		

a. Statistical Results

Table 9 outlines the variables selected and associated statistics for both thresholds. At best, these models explained only 38 percent of the variance in 6-hr rainfall (a correlation coefficient of 0.61). Both produced standard errors of about 0.6 in. Neither produced results better than the Eloise situation previously discussed.

Table 9 -- Results of the stepwise regression of 6-hr rainfall in the Missoui situation - 2200-0400 GMT, 25 and 26 August 1975.

STEP	-20°C N = 152			0°C N = 152		
1	10	20.5	.64	10	22.5	.63
2	17	26.1	.62	25	29.2	.60
3	7	28.5	.61	17	37.5	.57
4	21	31.9	.59	15	40.0	.55
5	15	33.7	.58	26	41.3	.55

Although variable 10 (IR temperature along the 850 mb wind) was, when using either threshold, the most highly correlated with rainfall, it was only weakly correlated at less than 0.5. Table 10 shows that of the other variables selected by either choice of thresholds, some were only slightly less well correlated with rainfall and may have served nearly as well had they been the first choice. Variable 7 may be a poor supplemental choice to variable 10 in the cold model since the two variables are so highly correlated. Others of the selected variables show such poor correlation to rainfall that they must be of questionable realism in the equations. Table 10 also indicates that all IR-related variables are poorly or virtually unrelated to rainfall. In contrast to the results of the Eloise cases, variables 2 and 11 (especially 2) appear to be unimportant to rainfall estimation. (Although not presented here, a table for the -20° threshold shows similar correlations which then permitted the use of table 10 instead.)

As might be expected from the foregoing results, a test of the 0°C-threshold using dependent data shows a very poor estimation of rainfall (figure 13). The estimation field is flat compared to the observed rainfall.

Examination of relationships to hourly rainfall proved just as unfruitful (table 11). Just as in the Eloise case selected variables either varied wildly or changed ranking from hour to hour. Models in any given hour explained no more than 46 percent of the variance and as little as 26 percent.

Table 10 -- Correlation table, 6-hr Missouri situation using the 0°C threshold.

	1	2	3	4	5	6	7	8	9	10	11	15	17	21	25	26
1	1.00															
2	-.09	1.00														
3	.08	.60	1.00													
4	.01	-.20	.13	1.00												
5	-.09	.27	.06	-.38	1.00											
6	-.19	-.51	-.46	-.04	-.12	1.00										
7	-.31	-.57	.54	-.05	-.10	.83	1.00									
8	-.28	-.14	-.12	-.01	-.07	.82	.50	1.00								
9	.34	-.14	.29	.17	-.07	-.86	-.66	-.84	1.00							
10	.47	.20	.36	.17	-.06	-.68	-.88	-.49	.75	1.00						
11	.34	-.05	.05	.09	-.04	-.71	-.39	-.92	.90	.52	1.00					
15	.07	-.17	.04	-.03	-.03	.50	.27	.48	-.41	-.18	-.38	1.00				
17	.42	-.06	-.17	-.04	-.02	-.11	-.33	-.03	.13	.44	.03	-.04	1.00			
21	.39	.10	.06	-.06	.06	-.31	-.41	-.26	.27	.40	.23	-.16	.39	1.00		
25	-.08	.57	.27	.07	.02	-.28	-.49	.06	.13	.38	-.14	-.03	.29	-.17	1.00	
26	-.01	.40	.33	-.07	.18	-.31	-.21	-.27	.11	-.01	.16	-.21	-.50	.23	-.23	1.00

Table 11 -- Results of the stepwise regressions for each hour of the Missouri situation using the 0°C threshold.

	23 GMT	00	01	02	03	04
STEP	N=113	N=120	N=126	N=136	N=148	N=152
1	10 17.3 .22	22 20.4 .13	21 18.7 .23	20 15.9 .25	20 14.8 .22	24 22.7 .21
2	13 29.9 .21	26 26.6 .13	17 22.9 .23	2 38.1 .22	2 25.9 .20	2 31.5 .20
3	5 36.0 .20	2 30.2 .13	23 26.5 .22	21 45.0 .20	11 32.9 .19	11 35.4 .19
4	23 39.6 .19	7 34.0 .12	2 29.6 .22	6 48.2 .20	18 36.6 .19	16 37.0 .19

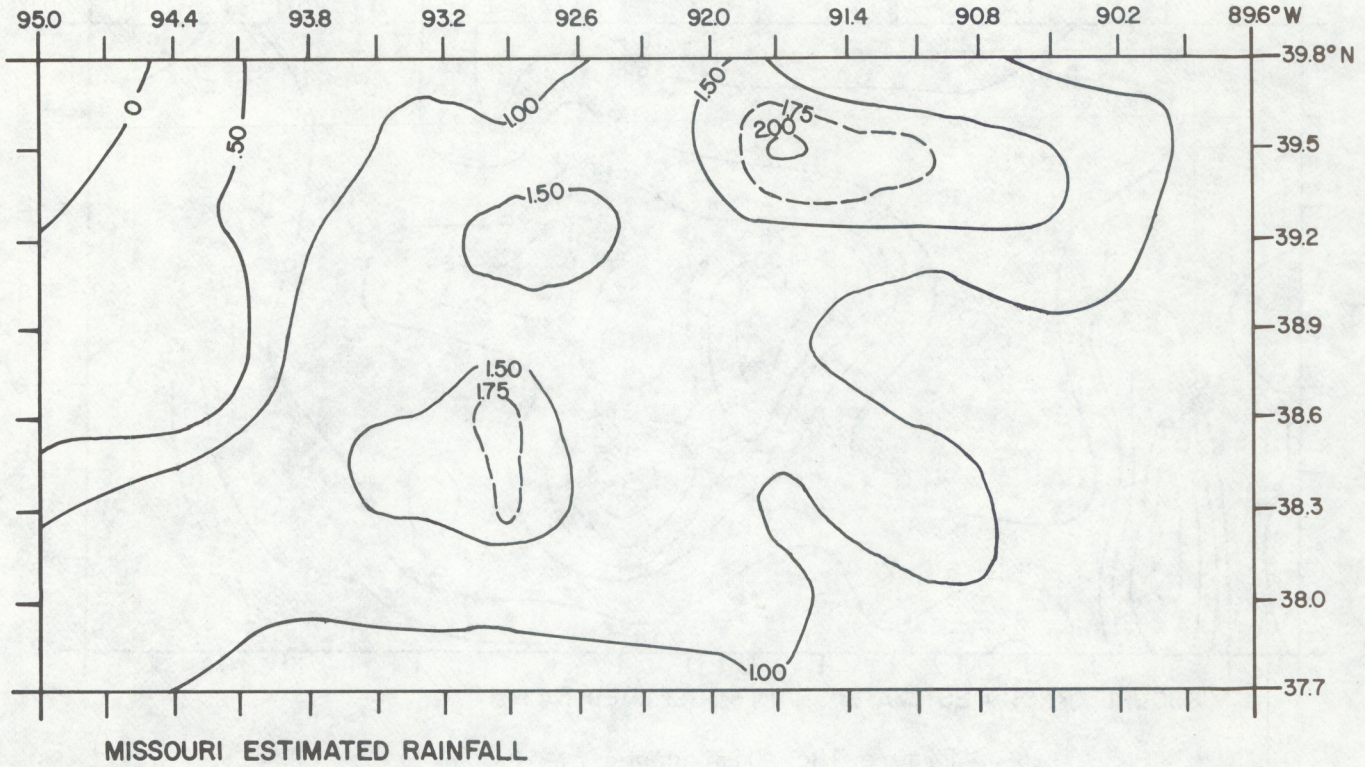

Figure 13a Estimated 6-hr rainfall in the Missouri case of 2200-0400 GMT, 25 and 26 August 1975. Variables 10, 25, and 17 were involved.

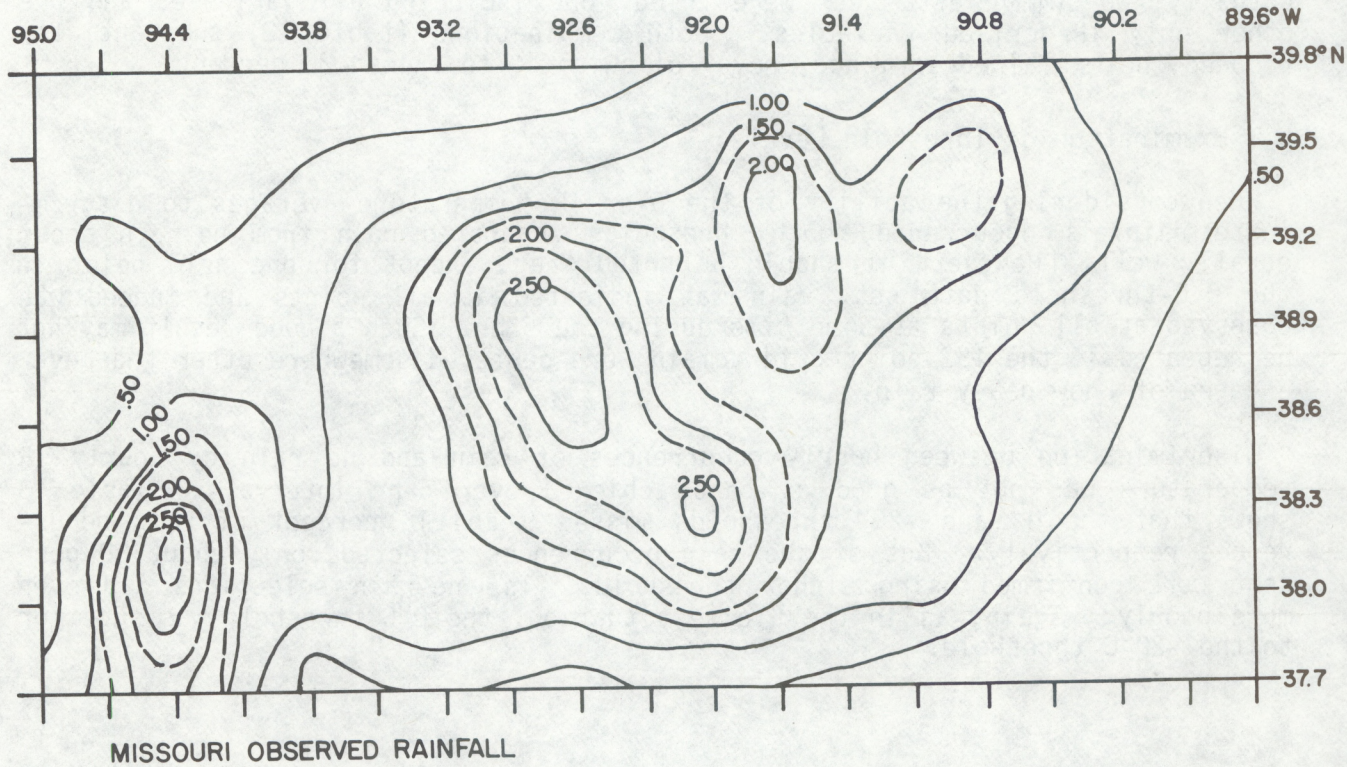

Figure 13b Observed rainfall for the same period.

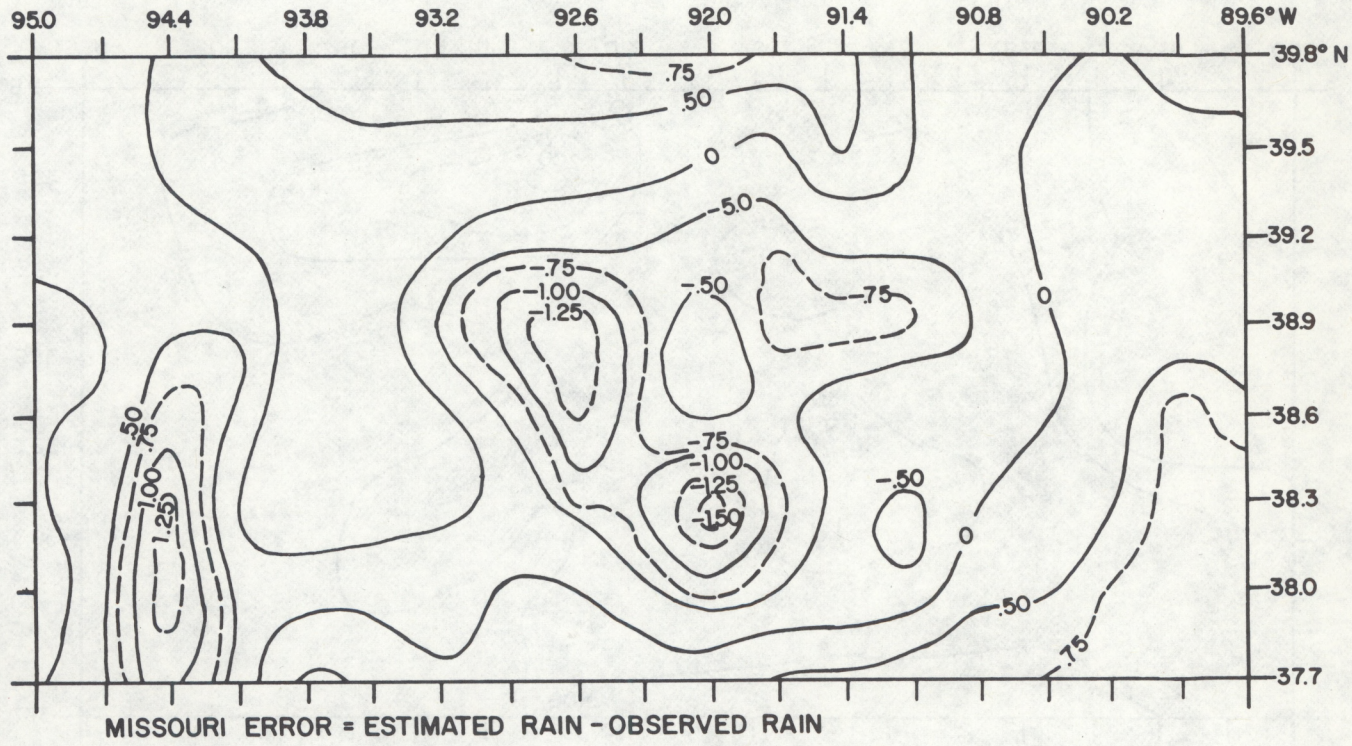

Figure 13c Difference of 13a and 13b.

No improvement was achieved by combining all hours into a common data set. Actually two common data sets were tried, one including all variables and the other only IR-derived variables. Both combinations (table 12) substantially reduced the explained variance, never allowing it to exceed 20 percent.

b. Examination of Threshold Levels.

When considering the ability of the 6-hr IR temperature averages to discriminate rainfall occurrence, both thresholds separated rain from no-rain about equally well. However, it should be noted that, except for one grid point in the 0^{o}C-threshold data set, rain was indicated at all points and indeed was observed at all points at some time during the 6 hr. Such a good result may not be repeated if the 152-point grid domain were centered somewhere other than over an area of know heavy rain.

Discrimination between hourly occurrences of rain and no rain by hourly IR temperature was not as good as that achieved over 6-hr intervals. Table 13 shows that the 0^{o} and -20^{o} thresholds missed 9 and 16 percent of rain occurrences respectively. But of the rain occurrences selected, only about 80 percent were confirmed using either threshold. The no-rain selections did even more poorly. Again, as in the Eloise situation, the 0^{o}C threshold was superior to the -20^{o}C threshold.

Table 12 -- Results of the stepwise regression of the combined hourly data in the Missouri situation using the 0°C threshold. Selections made from all variables and only IR variables are shown.

	ALL	IR
STEP	N=795	N=795
1	10 8.3 .23	10 8.3 .24
2	2 15.5 .22	2 15.5 .22
3	20 18.3 .22	4 16.9 .22
4	4 19.7 .22	5 17.3 .22

Table 13 -- Contingency tables of observed vs estimated instances of hourly rain (R) and no rain (NR) in the Missouri situation of 2230-0330 GMT, 25-26 August 1975.

a. 0°C THRESHOLD

OBSERVED	ESTIMATED R	ESTIMATED NR	TOTALS	OBSERVATIONS CORRECTLY ASSESSED
R	635	59	694	91%
NR	160	58	218	27%
TOTALS	795	117	912	
EST. COR.	80%	50%		

b. 20°C THRESHOLD

OBSERVED	ESTIMATED R	ESTIMATED NR	TOTALS	OBSERVATIONS CORRECTLY ASSESSED
R	582	110	692	84%
NR	144	76	220	35%
TOTALS	726	186	912	
EST. COR.	80%	41%		

5. SUMMARY AND CONCLUSIONS

Two very different convective situations have been examined statistically in an effort to develop an objective means of estimating rainfall from a number of satellite and conventional meteorological variables. In general, the statistical results revealed inconsistency in the variables selected, low correlations especially as cases were combined, inability to accurately reproduce rainfall fields from the regression models even using dependent data, and large, patterned scatter by the models employed.

Inconsistency of selected variables was well demonstrated in the Eloise situation by the nonrepetitive nature of the selected variables (or models) from one study area to another both at the same or different times and in the same area at different times. Low correlations were noted in the 6-hr case covering the Missouri squall line situation and in the Eloise situation, especially when several 6-hr cases were combined. Inconsistency was still worse among the hourly cases in both situations, and the correlations were lowest among the Missouri hourly cases. Even if the results from the hourly studies are dismissed because of small sample size, the results of the 6-hr cases cannot be so dismissed.

Despite the overall inconsistency among the 6-hr cases in the Eloise situation, when all cases were combined, two variables - IR temperature and the IR-temperature gradient along the shear - emerged to explain nearly 50 percent of the variance among the 0^{o}C-threshold data set and 38 percent among the -20^{o}C set. Though weak, these results afforded, for a time, one of the few positive notes of the study. It supported the physical reasoning that rain would be related to the coldest cloud tops and would be found near the upwind end of convection. It was also a surprising result since the convection in Eloise, though identifiable, was more diffuse and more shallow than that found even in most modest thunderstorms, thereby suggesting the possibility that rain amount might be estimated in clouds of less dramatic appearance. Nevertheless, tests of both models on dependent cases showed the rain amount to be severely underestimated in areas of heavy rain and the errors to be often 50 percent higher or lower than observed rain. There is little doubt that applying the equation to independent data, even from a similar meteorological situation, would produce worse results or that including more data into the regression analysis would explain less variance.

IR temperature showed virtually no correlation with rainfall in the Missouri situation. This negative result was as surprising as the more positive one in Eloise. Both were surprising since one normally expects rainfall definition by IR temperature to be more acute in a sharply defined convective situation than in a poorly defined one. Concern over this point is probably misplaced in view of the more important finding that neither IR temperature nor any of the variables derived from it was shown by this study to have a strong relationship to rainfall. Neither did any of the variables from conventional data appear to be strongly related to rainfall. Multivariate combinations provided limited improvement. Combined hourly relationships were even worse. Given these facts, the conclusion is clear: the statistical approach offers little ability to estimate rainfall, even area-averaged rainfall, with anything but extreme crudeness and certainly not to the accuracy required in hydrologic models.

Why the method failed is a disturbing question. Most of the IR guidelines for estimating rainfall were objectively examined. These included the possible relationships of IR temperature, coldest towers, and upwind portions of convective

debris to rainfall amount. Other variables, those more conventional in nature and normally associated with rain, were also included but to little avail.

So, what considerations and problems are involved which may have some bearing on these results? Two other variables which might have helped are radar intensity and cloud growth. Both are thought to be related to rainfall intensity, but both present problems to a study of this type. Accuracy of the observed rainfall is always a problem in itself. In order to avoid its high variability in the horizontal, an averaging technique was employed here which might well be inferior to some other. But, no matter what the technique, its reliability will always be adversely affected by sparse data networks.

Computer digitized radar data were avoided since they are available at only four widely separated sites. And, lacking overlaping coverage, no radar has the range to cover even the limited area used here unless perhaps it were coincidentally located at the center of the study area. Manually digitized radar was avoided upon advice that the subjective judgement involved renders it too variable and inconsistent for other than qualitative use.

Cloud growth was not employed for several reasons. By purely objective means, and sometimes by subjective means, it is difficult enough to simply separate distinct clouds. Moreover, even if growth is measured by some means, as for instance the areal change within a selected IR isotherm, there are questions about exactly where an increase in rainfall is expected, how a single value representing growth over a large area is applied to individual grid points, and how it is incorporated in a regression procedure involving many grid points. With the advent of overlapping coverage by computer-digitized radars and with more experimentation on the problem of measuring cloud growth, perhaps these variables could be included in a statistical approach.

Areal averaging of rainfall may have inadvertently introduced a statistical problem as well. It could have caused a dependence of rainfall at each grid point on other points nearby, thus destroying the greater independence of point-rainfall measurements. Point measurements are here assumed to have greater independence by virtue of the high variability of convective rainfall. Indeed, the tendency for error to increase with increasing amount of estimation, as noted in this study, indicates that the data do suffer from some sort of nonrandom characteristics. If the rainfall averaging process is at fault, then the effort here will have gone full circle. (It was introduced in the first place to overcome the poor correlation of point rainfall with IR temperature noted in a preliminary study of Eloise.) Although the correlation with IR temperature appears to have been improved in the Eloise situation by area averaging, all statistical models derived in both situations do suffer from patterned scatter whether or not IR temperature is a component of the model.

To make all data truly independent, many widely scattered samples in both space and time would have to be collected. Such an undertaking would be a monumental task compounded by the fact that several such data sets would probably be needed to properly represent variations in convective type, meteorological condition, season, climatology, terrain, etc.

The results presented here do not really support such an undertaking. In fact, at the very least, the results argue strongly against a statistical approach to rainfall estimation; at most, they raise concern about the validity of using the variables tested here to estimate rainfall.

One encouraging aspect of this study was that IR temperature showed an ability to discriminate instances of rain from no rain. Of the two threshold temperatures used, $0^{o}C$ was superior to $-20^{o}C$ and performed well. This result is tempered by the fact that all cases were bound to be favorably biased to some degree. The cases were selected in the first place based on their very active convection and rainfall; these characteristics, together with their being in rather confined areas (about the size of Pennsylvania), tend to insure a high incidence of rain. Given a less intense or less active situation, but one with reasonably deep (cold) convective clouds, an entirely different result may occur. At any rate, this point needs further investigation.

ACKNOWLEDGMENTS

Particular appreciation is expressed to Leroy D. Herman who did all of the initial programming connected with this project. Special thanks are due to Thomas I. Babicki who, later in the project, assumed responsibility for the running and upkeep of all the programs and changed and combined programs to simplify the computer processing. Also, special thanks are given to John A. Booth who gave the author cooperative assistance throughout and to Edward King who did the drafting. Appreciation is also given for the interest of Richard K. Farnsworth of the Office of Hydrology who gathered and provided the rainfall data and who, along with Ray Canterford, visiting scientist from the Australian Bureau of Meteorology, followed the progress of the project and offered encouragement and helpful suggestions. Thanks are also expressed to Myron W. Gwinner of the Harrisburg, Pennsylvania RFC for furnishing precipitation averages of drainage basins and for explaining the realities of collecting and averaging rainfall and of modeling riverflow. Thanks are also given to Carroll A. Maunder for not only typing the manuscript but for undergoing the "hassle" of scheduling and waiting for time on the word processor.

REFERENCES

Arkin, P. A., 1979: The relationship between fractional coverage of high cloud and rainfall accumulations during GATE over the B-scale array. Mon. Wea. Rev., 107, 10, 1382-1387.

Barrett, E. C., 1970: The estimation of monthly rainfall from satellite data. Mon. Wea. Rev., 98, 4, 322-327.

Follansbee, W. A., 1973: Estimation of average daily rainfall from satellite cloud photographs. NOAA Tech. Memo, NESS 44, National Environmental Satellite Service, NOAA, Washington, D. C., 39 pp.

Griffith, C. G., W. L. Woodley, P. G. Grube, D. W. Martin, J. Stout, and D. N. Sikdar, 1978: Rain estimation from geosynchronous satellite imagery -- visible and infrared studies. Mon. Wea. Rev. 106, 8, 1153-1171.

Gruber, A., 1973: Estimating rainfall in regions of active convection. J. Appl. Meteor., 12, 1, 110-118.

Hydrologic Research Laboratory, 1972: National Weather Service river forecast system forecast procedures. NOAA Tech. Memo NWS HYDRO-14. National Weather Service, NOAA, Washington, D. C., 77 pp. and 9 append.

Lethbridge, M., 1967: Precipitation probability and satellite radiation data. Mon. Wea. Rev., 95, 7, 487-490.

Maddox, R. A., C. F. Chappell, and L. R. Hoxit, 1979: Synoptic and meso-scale aspects of flash flood events. Bull. Amer. Meteor. Soc., 60, 2, 115-123.

Miller, R. C., 1972: Notes on analysis and severe-storm forecasting procedures of the Air Force Global Weather Central. Technical Report 200 (rev.) Air Weather Service, U. S. Air Force, 98 pp., 8 Append.

National Climatic Center, 1975: Storm Data. NOAA monthly publication, Environmental Data and Information Service, NOAA, Asheville, N. C.

Scofield, R. A. and Oliver, V. J., 1977: A scheme for estimating convective rainfall from satellite imagery. NOAA Tech. Memo, NESS 86, National Environmental Satellite Service, NOAA, Washington, D. C., 47 pp.

APPENDIX A

Variable 1 - Area averaged rainfall, R

This variable, the predictand of the study, is area-averaged rainfall as determined from the 1-hr rain-gauge network for periods of either 6-hr or 1-hr. An analysis program "Weaver" (appendix C) determined the rainfall at 0.1 deg intervals over the analysis area and some 1.0 deg beyond 3 x 3 arrays of these values centered at each grid point were then averaged to obtain the average rainfall over each 0.3-deg grid box.

Variable 2 - IR Temperature, C

The coldest tops of convective clouds are presumed to bear some relation to rainfall. IR radiation values are readily converted to temperature by means of the standard calibration table which makes the assumption that the clouds are radiating as black bodies and thus have an emissivity of 1. For purposes of this study, temperature means are taken from a cluster of 27 values centered on each grid point. These clusters are arrays of three lines by nine pixels. Generally, to achieve an undistorted perspective, a line width is about equivalent to 21/4 pixel widths. Means are taken for three reasons: to minimize the adverse effects of noise in the data, to achieve an areal rather than point basis of comparison, and to reduce navigational (gridding) inaccuracies.

For purposes of segregating cold clouds from warm targets, a threshold temperature is used. During the averaging process, any temperature above the threshold is set at the threshold level in order to minimize the effect of warm targets, especially those much warmer than the threshold. Two thresholds are used in this study, $-20^{\circ}C$ and $0^{\circ}C$. Only if the mean temperature is below the threshold value is rain presumed to have occurred and the associated grid point included in the statistical calculations. IR temperature then enters into the study twice; first, in determining the locations of rain occurrence and second, as a potential variable for determining amount of rain. When hourly rainfall is under study, areal averages from a single representative image are used; for 6-hr, the areal averages of all six images are averaged as well.

Variable 3 - Absolute Gradient of IR Temperature, $|\nabla C|$

Sharp gradients internal to convective cloud tops are often found near the highest towers and thus rain might well be associated with them. To calculate these gradients, the four arrays (each is three lines by nine pixels) adjacent to the four sides of each temperature array used in variable 2 is selected and averaged. The five-point array of IR temperatures thus created forms the structure for calculating all of the IR-related variables. Gradient is determined in the usual fashion by taking differences across the grid point along perpendicular paths by the equation,

$$|\nabla C| \approx \sqrt{\left(\frac{C_2 - C_4}{2\Delta X}\right)^2 + \left(\frac{C_1 - C_3}{2\Delta Y}\right)^2},$$

where C is temperature, the subscripts refer to the four points around the grid point, and $2\Delta X$ and $2\Delta Y$ are the Earth distances between temperature locations along the scan line and across the scan lines, respectively. Absolute value of

the gradient is used since it was the strength of the gradient being sought and not the direction or sign.

Because of foreshortening caused by the Earth's curvature and variable slant range to each earth point, the resolution of each picture element or pixel varies over the satellite scene of view. As a result, the earth distances $2\Delta X$ and $2\Delta Y$ above are different for every such interval over the scene. These distances are calculated at each gridpoint in order to avoid any adverse effects on the statistics. The equations involved are:

$$\Delta X = \{(|i\cos\alpha| + |j\sin\alpha|)|\cos\psi| + (|i\sin\alpha| + |j\cos\alpha|)|\sec\beta\sin\psi|\} \times \left|\frac{D+r}{D}\csc\beta\sin[\cos^{-1}(\cos\Delta\phi\cos\theta)]\right|$$

and

$$\Delta Y = \{(|i\sin\alpha| + |j\cos\alpha|)|\sec\beta\cos\psi| + (|i\cos\alpha| + |j\sin\alpha|)|\sin\psi|\} \times \left|\frac{D+r}{D}\csc\beta\sin[\cos^{-1}(\cos\Delta\phi\cos\theta)]\right|$$

where θ = latitude of the gridpoint and is known from navigation,

$\Delta\phi$ = longitudinal separation between gridpoint and satellite subpoint and is known from navigation.

$\alpha = \tan^{-1}[\sin\Delta\phi\,\mathrm{ctn}\,\theta]$ and is the azimuth to the gridpoint from the subpoint,

$\beta = \tan^{-1}\left[\frac{\sin\{\cos^{-1}(\cos\Delta\phi\cos\theta)\}}{\cos\Delta\phi\cos\theta - r/D+r}\right]$ and is the angle between the image and Earth tangent plain at the grid point,

$\psi = \tan^{-1}\left[\frac{\tan\Delta\phi}{\sin\theta}\right]$ and is the angle formed by the longitude of the gridpoint and the great circle arc to the subpoint from the grid point,

i = product of the pixel count along scan line and the subpoint resolution of the line divided by the aspect ratio (pixels to scan lines) which is 9X3.703/2.27 = 14.68 nmi and is the subpoint resolution of nine pixels,

j = product of the line count and subpoint resolution of the line which is 3 x 3.703 = 11.11 nmi and is the subpoint resolution of three scan line widths,

r = 3,437.87 nmi and is radius of the Earth,

and

D = satellite height above the surface of the Earth and is known from orbital elements.

Variable 4 - Laplacian of IR temperature, $\nabla^2 C$

This variable offers the possibility that the cold convective towers normally associated with rain might be identified without regard to the actual IR temperature. Temperature arrays described in variable 2 were used to calculate the lapacian of IR temperature according to

$$\nabla^2 C \approx \frac{C_2 + C_4 - 2C_5}{(\Delta X)^2} - \frac{C_1 + C_3 - 2C_5}{(\Delta Y)^2} ,$$

where symbols have the same meaning as before and the subscript 5 refers to the grid point location.

Variable 5 - Ratio of the IR temperature to lapacian of IR temperature, $\nabla^2 C/C$

This variable is an index intended to show whether the coldest towers are best related to rainfall. It is derived by forming the ratio of variable 4 to variable 2.

Variable 6 - IR temperature gradient along 200 mb wind, $\mathbf{V}_2 \cdot \nabla C / |\mathbf{V}_2|$

If rain is to be expected near the convective towers, then perhaps some particular portion of the main cloud area is more frequently associated with rain than others. For instance, cold convective debris carried far downstream usually produces little rain. It is reasoned therefore that, by measuring the cloud-top temperature gradient along various wind directions, the storm can be partitioned by gradient to learn whether any relationship to rain exists. Because of the downstream spread of convective debris, large positive gradients of temperature may occur just upstream of towers, small negative gradients downstream, and small gradients across stream. The gradient is calculated by

$$\frac{\mathbf{V}_2 \cdot \nabla C}{|\mathbf{V}_2|} \approx -\frac{C_2 - C_4}{2\Delta X} \sin\delta - \frac{C_1 - C_2}{2\Delta Y} \sin\delta$$

where $\mathbf{V}_2$ is the 200 mb wind vector, δ is the wind direction, and all other symbols have the same meaning as in the discussion of variable 2.

Variable 7 - IR Temperature gradient along 850 mb wind, $\mathbf{V}_8 \cdot \nabla C / |\mathbf{V}_8|$

Logic similar to that outlined in variable 6 is used to design this variable but with the intent to partition the cloud differently. The lower tropospheric wind, if in the normal counterclockwise orientation relative to the high-level wind, may identify a large positive gradient on the right flank (usually south) of the towers, a large negative gradient on the left flank (north), and weaker gradients across stream of the towers but possibly somewhat stronger to the left.

Variable 8 - IR temperature gradient along the tropospheric shear, $\mathbf{V}_{2-8} \cdot \nabla C / |\mathbf{V}_{2-8}|$

This variable might be expected to identify a moderately strong positive gradient on the upshear side of towers somewhere in between that of the previous two variables. A moderately weak negative gradient might be found downshear of towers and rather weak gradients across shear. Vector differences of the previous two wind fields provide the shear direction for this analysis.

Variables 9, 10, and 11 - IR Temperature and gradients combined, $C \mathbf{V} \cdot \nabla C / |\mathbf{V}|$

These are variables 6-8 modified as a product with variable 2. This approach is predicated on the premise that the strongest gradients in the coldest portions of the storm might have a better relation to rain than either alone.

Variables 12 and 13 - Surface Dewpoint, DP_{SFCM} (midtime), DP_{SFCS} (start)

Surface dewpoint, being a measure of low-level moisture, is potentially related to rainfall. This dewpoint analysis and all meteorological analyses in this study were done by the Thomasell scheme. Midtime and start time refer to the 6-hr intervals of study. An explanation of these times is given in section 3.

Variable 14 - 850 mb dewpoint available by midtime, DP_8

This, just as surface dewpoint, is another measure of low-level moisture and therefore potentially related to rainfall, especially to convective rainfall. (See also section 3.)

Variables 15 and 16 - Advection of surface dewpoint (start and midtime) by the 850 mb wind available at midtime, $-\vec{V}_8 \cdot \nabla DP_{SFCS}$, $-\vec{V}_8 \cdot \nabla DP_{SFCM}$

The rate at which low-level dewpoint is being transported into an area seems at least as likely to be related to convective rain as moisture itself. Analyses of 850 mb wind from variable 7 and gradients of surface dewpoint analysis from variables 12 and 13 are used in these calculations. Because of the often irregular behavior of surface winds due to terrain effects, the 850 mb wind is used instead.

Variable 17 - Advection of 850 mb dewpoint by the 850 mb wind available by midtime, $-\vec{V}_8 \cdot \nabla DP_8$

This variable is designed, just as are variables 15 and 16, to be a measure of the low-level moisture being transported into an area and therefore possibly related to rainfall.

Variables 18 and 19 - Gradient of surface dewpoint at both midtime and start time along the 200 mb wind available at midtime, $\vec{V}_2 \cdot \nabla DP_{SFCM} / |\vec{V}_2|$, $\vec{V}_2 \cdot \nabla DP_{SFCS} / |\vec{V}_2|$

In severe storm forecasting, the high-level windward side of the low-level moist tongue is regarded as a likely place for intense convection (Miller, 1972). Although this factor has not been specifically related to rain as it has to other severe storms such as tornadoes, it is included among the variables of this study. This gradient determination is made using dewpoint analyses derived in variables 12 and 13 and the wind analysis derived in variable 6.

Variable 20 - Gradient of 850 mb dewpoint along the 200 mb wind, $\vec{V}_2 \cdot \nabla DP_8 / |\vec{V}_2|$

The rationale for the design of this variable is the same as that in variables 18 and 19. Gradient determination is made using the dewpoint analysis derived in variable 14 and the wind analysis in variable 6.

Variable 21 and 22 - Laplacian of surface dewpoint at midtime and start time, $\nabla^2 DP_{SFCM}$, $\nabla^2 DP_{SFCS}$

This variable should identify relative maxima and minima of low-level moisture which may correlate better with rain than an absolute measure of moisture. Calculation is made from the analysis of variable 12 or 13.

Variable 23 - Laplacian of 850 mb dewpoint available at midtime, $\nabla^2 DP_8$

Design of these variables is based on the same rationale as that in variables 21 and 22. Calculation is made from the analysis of variable 14.

Variables 24 and 25 - Equivalent potential temperature at midtime and at start time, θ_{eM}, θ_{es}

Better than moisture alone, equivalent temperature combines low-level effects of both heat and moisture and may better define instability and thus convective potential. Surface dewpoint, temperature, and pressure at both midtime and start time of the 6-hr rainfall period are used.

Variable 26 - Height of terrain, h

High terrain is often thought to experience more rain than low terrain. This variable is then included, even though it is recognized that absolute height may not itself relate well to rain. Relatively high terrain might correlate better with rain and is defined by the next two variables. Terrain height is defined here by an analysis of the height of the rain-gage stations.

Variable 27 - Gradient of terrain height along the 850 mb wind, $\mathbf{V}_8 \cdot \nabla h / |\mathbf{V}_8|$

This variable identifies up-slope motion in association with rainfall. It is calculated using the terrain height of variable 26 and the wind field from variable 7.

Variable 28 - Laplacian of terrain height, $\nabla^2 h$

This variable should separate higher from lower terrain. The higher terrain may be associated with heavier rainfall. It is calculated from the analysis obtained in variable 26.

APPENDIX B

Density by State of Daily-Observing
and Hourly-Observing Precipitation Stations

	DAILY STATIONS[7]	HOURLY STATIONS[7]	STATE AREA	AREA PER DAILY STA.	AREA PER HOURLY STA.	AVERAGE SPACING DAILY STA.	AVERAGE SPACING HOURLY STA.
			(sq mi)	(sq mi)	(sq mi)	(mi)	(mi)
ALABAMA	148	32	51,609	348.7	1612.8	18.7	40.1
ARKANSAS	63	54	53,104	842.9	983.4	29.0	31.4
CONNECTICUT	39	18	5,009	128.4	278.3	11.3	16.7
DELAWARE	9	3	2,058	228.7	686.0	15.1	26.2
GEORGIA	156	56	58,876	377.4	1051.4	19.4	32.4
INDIANA	112	75	36,291	324.0	483.9	18.0	22.0
ILLINOIS	166	74	56,400	339.8	762.1	18.4	27.6
IOWA	152	75	56,290	370.3	750.5	13.2	27.4
KANSAS	272	72	82,264	302.4	1142.6	17.4	33.8
KENTUCKY	152	54	40,395	265.8	748.1	16.3	27.4
LOUISIANA	134	36	48,523	362.1	1347.9	19.0	36.7
MARYLAND	75	16	10,577	141.0	661.1	11.9	25.7
MICHIGAN	153	55	58,216	380.5	1058.5	19.5	32.5
MISSISSIPPI	144	52	47,716	331.4	917.6	18.2	30.3
MISSOURI	215	102	69,686	324.1	683.2	18.0	26.1
NEBRASKA	175	58	77,227	441.3	1331.5	21.0	36.4
NEW JERSEY	54	19	7,836	145.1	412.4	12.0	20.3
NEW YORK	266	86	49,576	186.3	576.5	13.7	24.0
NORTH CAROLINA	175	48	52,712	301.2	1098.2	17.4	33.1
OHIO	184	95	41,222	224.0	433.9	15.0	20.8
OKLAHOMA	186	72	69,919	375.9	971.1	19.4	31.2
PENNSYLVANIA	287	136	45,333	158.0	333.3	12.6	18.3
SOUTH CAROLINA	97	25	31,055	320.2	1242.2	17.9	35.2
TENNESSEE	103	45	42,244	410.1	938.8	20.3	30.6
TEXAS	592	201	267,339	451.6	1330.0	21.3	36.5
VIRGINIA	150	44	40,815	272.1	927.6	16.4	30.4
WEST VIRGINIA	120	41	24,181	201.5	589.8	14.2	24.3

[7]Numbers obtained from Climatological Data and Hourly Precipitation Data, published by U. S. Department of Commerce, NOAA, Environmental Data and Information Service, Asheville, North Carolina.

APPENDIX C

WEAVER[8] Subroutine Applied to Average Rainfall Areally

This subroutine uses data values to prepare an underlying array AREA which may then be contoured.

CALL WEAVER 9VAL, NUMV, AREA, WAREA, IH, IV, XL, XR, XT, DIST, ILR, IBT, IWEAV, IDEC, IFINE, CENTR, ICHEKO.

In this explanation of WEAVER, points which are assigned values from the observed data are referred to as "observed" points and the others as "filled" points. A unit distance is the distance between orthogonally adjacent points. The program begins by establishing a first approximation field.

Initially observed data are assigned to the nearest grid point or "observed" point. Each point at the border of the grid which remains unfilled is given a value using observed points within a distance of eight units. The weight given to each observed point is one minus the normalized distance squared, i.e.: $w_i = 1-(d_i/8)^2$, where w_i is the weight and d_i is the distance in unit measure.

The value assigned is then $V = \Sigma (w_i V_i)/\Sigma w_i$, where the summation is taken over all observed points within eight units. If the sum of the weights is zero, the point is not filled. The process is then repeated on the borders, using both observed and filled border points as observed points, until the borders are completely filled.

The program then proceeds to complete the first approximation field by linear interpolation. Alternating vertically and horizontally, the program fills unfilled points using endpoints up to a chosen distance. The choice of the initial distance is the quantity DIST. It is based on the dispersion of observed points. If the grid cannot be filled with the distance allowed, then the distance is increased by the value of the original distance; however, it is never allowed to exceed half the length of the minimum dimension of the format.

After the first approximation field is established, the smoothing of values at the filled points begins.

On the first pass through the smoothing routine, the value at a filled point is revised as a function of both its own value and the values of the surrounding eight points. The weight at the four corner points is one over the square root of two. At the adjacent four points, the weight is one; for the point itself, the weight is the sum of the other weights which is 6.83. The weight at any

---

[1]Program and description obtained from Donald H. Flanders, NOAA Office of Management and Budget, Office of Management and Computer Systems.

observed point is modified to be the product of the original weight and 6.83; thereby, an adjacent observed point has the same weight as the point being filled. The new value of a point is then $V = \Sigma(w_i v_i)/\Sigma w_i$, with the sum being taken over the nine points. No point is revalued until the pass is completed. On the second pass, the four corner points are not considered. The four adjacent points are given a weight of one and the point itself has a weight of four. An observed point is reweighted at four. The new value is then determined as before.

If the call indicates that observed points are to be modified, the weights at surrounding points are determined as before, but the weight at an observed point is equal to the sum of the weights for surrounding points times the factor CENTR passed to the subroutine. At border points, the obvious modifications are made. The number of executions of the smoothing routine is determined by the parameter IFINE, with a minimum of two executions corresponding to a value of zero for IFINE.

(Continued from inside front cover)

NESS 61 The Measurement of Atmospheric Transmittance From Sun and Sky With an Infrared Vertical Sounder. W. L. Smith and H. B. Howell, September 1972, 16 pp. (COM-73-50020)

NESS 62 Proposed Calibration Target for the Visible Channel of a Satellite Radiometer. K. L. Coulson and H. Jacobowitz, October 1972, 27 pp. (COM-73-10143)

NESS 63 Verification of Operational SIRS B Temperature Retrievals. Harold J. Brodrick and Christopher M. Hayden, December 1972, 26 pp. (COM-73-50279)

NESS 64 Radiometric Techniques for Observing the Atmosphere From Aircraft. William L. Smith and Warren J. Jacob, January 1973, 12 pp. (COM-73-50376)

NESS 65 Satellite Infrared Soundings From NOAA Spacecraft. L. M. McMillin, D. Q. Wark, J.M. Siomkajlo, P. G. Abel, A. Werbowetzki, L. A. Lauritson, J. A. Pritchard, D. S. Crosby, H. M. Woolf, R. C. Luebbe, M. P. Weinreb, H. E. Fleming, F. E. Bittner, and C. M. Hayden, September 1973, 112 pp. (COM-73-50936/6AS)

NESS 66 Effects of Aerosols on the Determination of the Temperature of the Earth's Surface From Radiance Measurements at 11.2 m. H. Jacobowitz and K. L. Coulson, September 1973, 18 pp. (COM-74-50013)

NESS 67 Vertical Resolution of Temperature Profiles for High Resolution Infrared Radiation Sounder (HIRS). Y. M. Chen, H. M. Woolf, and W. L. Smith, January 1974, 14 pp. (COM-74-50230)

NESS 68 Dependence of Antenna Temperature on the Polarization of Emitted Radiation for a Scanning Microwave Radiometer. Norman C. Grody, January 1974, 11 pp. (COM-74-50431/AS)

NESS 69 An Evaluation of May 1971 Satellite-Derived Sea Surface Temperatures for the Southern Hemisphere. P. Krishna Rao, April 1974, 13 pp. (COM-74-50643/AS)

NESS 70 Compatibility of Low-Cloud Vectors and Rawins for Synoptic Scale Analysis. L. F. Hubert and L. F. Whitney, Jr., October 1974, 26 pp. (COM-75-50065/AS)

NESS 71 An Intercomparison of Meteorological Parameters Derived From Radiosonde and Satellite Vertical Temperature Cross Sections. W. L. Smith and H. M. Woolf, November 1974, 13 pp. (COM-75-10432)

NESS 72 An Intercomparison of Radiosonde and Satellite-Derived Cross Sections During the AMTEX. W. C. Shen, W. L. Smith, and H. M. Woolf, February 1975, 18 pp. (COM-75-10439/AS)

NESS 73 Evaluation of a Balanced 300-mb Height Analysis as a Reference Level for Satellite-Derived soundings. Albert Thomasell, Jr., December 1975, 25 pp. (PB-253-058)

NESS 74 On the Estimation of Areal Windspeed Distribution in Tropical Cyclones With the Use of Satellite Data. Andrew Timchalk, August 1976, 41 pp. (PB-261-971)

NESS 75 Guide for Designing RF Ground Receiving Stations for TIROS-N. John R. Schneider, December 1976, 126 pp. (PB-262-931)

NESS 76 Determination of the Earth-Atmosphere Radiation Budget from NOAA Satellite Data. Arnold Gruber, November 1977, 31 pp. (PB-279-633)

NESS 77 Wind Analysis by Conditional Relaxation. Albert Thomasell, Jr., January 1979.

NESS 78 Geostationary Operational Environmental Satellite/Data Collection System. July 1979, 86 pp. (PB-301-276)

NESS 79 Error Characteristics of Satellite-Derived Winds. Lester F. Hubert and Albert Thomasell, Jr. June 1979, 44 pp. (PB-300-754)

NESS 80 Calculation of Atmospheric Radiances and Brightness Temperatures in Infrared Window Channels of Satellite Radiometers. Michael P. Weinreb and Michael L. Hill, March 1980, 43 pp. (PB80 208-119)

NESS 81 Improved Algorithm for Calculation of UTM and Geodetic Coordinates. Jeff Dozier, September 1980, 21 pp. (PB81 132680)

NESS 82 The Effect of Precipitation on Microwave Soundings in Low Latitudes. Lester F. Hubert, Norman C. Grody, Andrew Timchalk, and William C. Shen, April 1981, 34 pp. (PB81 225062)

NESS 83 Atmospheric Sounding User's Guide. Adolf Werbowetzki, ed., April 1981, 82 pp. (PB81 230476)

NESS 84 Use of NOAA/AVHRR Visible and Near-Infrared Data for Land Remote Sensing. Stanley R. Schneider, David F. McGinnis Jr., James A. Gatlin, September 1981.

NESS 85 Transmittances for the TIROS Operational Vertical Sounder. M.P. Weinreb, H.E. Fleming, L.M. McMillin, and A.C. Neuendorffer, September 1981.

NESS 86 Statistical and Synoptic Evaluations of TIROS-N and NOAA-6 Retrievals. Harold J. Brodrick, Carmella Watkins, and Arnold Gruber, October 1981.

NESS 87 Satellite Observations of Variations in Northern Hemisphere Seasonal Snow Cover. Kenneth F. Dewey and Richard Heim, Jr. December 1981.

NESS 88 Observations of Hurricane David (1979) Using the Microwave Sounding Unit. Norman C. Grody and William C. Shen, March 1982. (In press.)

NOAA SCIENTIFIC AND TECHNICAL PUBLICATIONS

The National Oceanic and Atmospheric Administration was established as part of the D of Commerce on October 3, 1970. The mission responsibilities of NOAA are to assess the socioeco t of natural and technological changes in the environment and to monitor and predict the state of th , the oceans and their living resources, the atmosphere, and the space environment of the Earth.

The major components of NOAA regularly produce various types of scientific and techn - tion in the following kinds of publications:

PROFESSIONAL PAPERS — Important definitive research results, major techniques, and special investigations.

CONTRACT AND GRANT REPORTS — Reports prepared by contractors or grantees under NOAA sponsorship.

ATLAS — Presentation of analyzed data generally in the form of maps showing distribution of rainfall, chemical and physical conditions of oceans and atmosphere, distribution of fishes and marine mammals, ionospheric conditions, etc.

TECHNICAL SERVICE PUBLICATIONS — Reports containing data, observations, instructions, etc. A partial listing includes data serials; prediction and outlook periodicals; technical manuals, training papers, planning reports, and information serials; and miscellaneous technical publications.

TECHNICAL REPORTS — Journal quality with extensive details, mathematical developments, or data listings.

TECHNICAL MEMORANDUMS — Reports of preliminary, partial, or negative research or technology results, interim instructions, and the like.

Information on availability of NOAA publications can be obtained from:

ENVIRONMENTAL SCIENCE INFORMATION CENTER (OA/D812)
ENVIRONMENTAL DATA AND INFORMATION SERVICE
NATIONAL OCEANIC AND ATMOSPHERIC ADMINISTRATION
U.S. DEPARTMENT OF COMMERCE

Rockville, MD 20852

NOAA--S/T 82-26